International Journal of Theoretical and Applied Mathematics
2016; 2(2): 170-189
http://www.sciencepublishinggroup.com/j/ijtam
doi: 10.11648/j.ijtam.20160202.32
ISSN: 2575-5072 (Print); ISSN: 2575-5080 (Online)

Modeling and Simulation of Non-Linear and Hysteresis Behavior of Magneto-Rheological Dampers in the Example of Quarter-Car Model

Sulaymon L. Eshkabilov

Dynamics & Control Lab, Tashkent Institute of Automotive Road Design, Construction and Maintenance, Tashkent, Uzbekistan

Email address:
sulaymon@d-c-lab.com

To cite this article:
Sulaymon L. Eshkabilov. Modeling and Simulation of Non-Linear and Hysteresis Behavior of Magneto-Rheological Dampers in the Example of Quarter-Car Model. *International Journal of Theoretical and Applied Mathematics.* Vol. 2, No. 2, 2016, pp. 170-189.
doi: 10.11648/j.ijtam.20160202.32

Received: November 13, 2016; **Accepted**: December 2, 2016; **Published**: January 23, 2017

Abstract: This paper presents reviews of mathematical formulations and numerical simulation models of non-linear and dynamic hysteresis behaviors of magneto-rheological liquid dampers, viz. Bingham, Dahl, LuGre and Bouc-Wen models, developed in MATLAB®/Simulink® in the example of quarter-car model with the Golden Car parameters. It demonstrates numerical simulations of the magneto-rheological liquid damper models with different sets of parameters and discusses simulation results and performances of these four models for different road profile excitation signals, such as Heaviside step function, sine wave, random noise and white Gaussian noise.

Keywords: Suspension, Bingham, Dahl, LuGre, Bouc-Wen, MATLAB/Simulink

1. Introduction

Most of the natural phenomena, operational machine processes and dynamic system behaviors are of non-linear nature that is very often linearized for the sake of simplicity in formulations and analyses. In fact, nonlinear behaviors or phenomena of processes may create difficulties in studies, engineering design processes and control applications but considering some of those non-linear characteristics of processes or behaviors of dynamic systems carefully could be also very beneficial and of great practical importance for efficient and accurate control, and used for operational efficiency and energy preservation, or on the contrary, energy dissipation depending on their application areas. For example, nonlinear parameters and characteristics of some materials and interactions of different parts made of different materials have a great potential to apply for dampers and shock absorbers [1]. One of the good examples for such processes is a hysteresis loop observed in magnetic or magnetized materials and magneto-rheological (MR) liquids. In experimental studies of [2], the MR liquid composition and its application for brakes have been studied, and found effects of metallic particle sizes on efficiency of temperature dissipation and efficient braking. In studies [3, 4, 5, 6], the MR liquids are found to be very suitable and promising in designing vibration dampers and shock absorbers, and there are some combinatorial designs [7] of the MR fluid dampers. One of the most attractive features of the MR fluids for dampers is that these liquids can operate in wide range temperatures from -40°C up to 150°C [8]. The MR dampers may have linear characteristics, that is viscous liquid properties, and can be switched easily from that state to a non-linear hysteresis or semi-solid (non-Newtonian liquid) flow state, that process can be controlled with a relatively low voltage values, i.e. 5V. Because of these features, the MR liquids have become very attractive research area, in particular in vibration damping. The valuable properties of hysteresis type fluids have been a subject of considerably profound studies and well formulated analytical models, viz. Bingham [9], Dahl [10], LuGre [11, 12] and Bouc-Wen [13, 14, 15], have been developed and there are many studies in alternative, extended and improved formulations of these models and their practical applications. For instance, in studies [16], feasibility of the MR liquid damper modeled by employing the Bouc-Wen model in association with an intelligent self-tuning PID controller for semi-active suspension modeling is studied numerically via computer modeling in

MATLAB®/Simulink®. Nevertheless, identification of the hysteresis loop parameters is rather complex and may require considerable laboratory and numerical studies in order to apply them and get a best use of the MR damper properties.

In this paper, we put some emphases on four different mathematical models and formulations of the MR liquid dampers, viz. Bingham, Dahl, LuGre and Bouc-Wen models, and their computer models and numerical simulations. In addition, we perform comparative analyses of these models in terms of their formulations and performances in damping undesired excitations from terrain roughness. For this purpose, we demonstrate comparative studies of hysteresis loop parameters of the MR liquid damper models and their influence on the model performances in terms of efficiency and responsiveness. The computer simulation models of the four models are developed for a semi-actively controlled feedback damper of a vehicle suspension system in MATLAB®/Simulink® and performances of these models are compared against the passive suspension model. In addition, we analyze and compare efficiency and responsiveness of these models in the example of the quarter-car model in order to design a semi-active suspension system (based on the Golden car parameters) capable of providing comfort ride. We carry out a few numerical simulation studies with various reference input signals expressing road profile irregularities as a function of time.

2. Mathematical Formulation of a Quarter-Car Model

To derive an equation of (vertical) motion of a vehicle induced by terrain irregularities, we consider a quarter car model by assuming that terrain roughness is evenly distributed under all wheels of a vehicle and loading from the whole vehicle body is equally distributed across all of its axles. In addition, we consider that a tire has small damping effect. With these preconditions, we draw the next physical model (Figure 1) of the system for passively and semi-actively controlled systems of a quarter-car model.

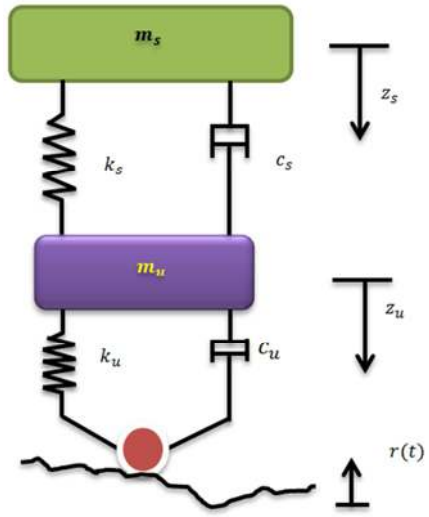

a) Passive suspension design

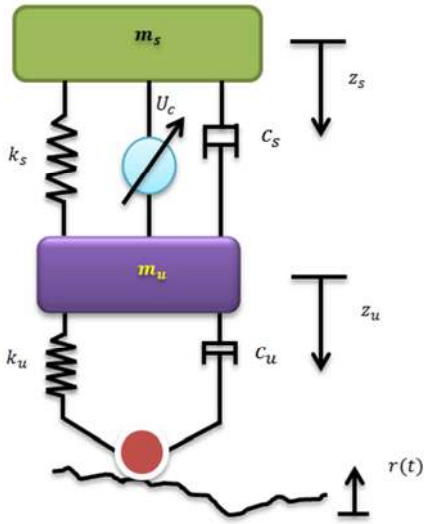

b) Semi-active suspension design

Figure 1. *Quarter-car models.*

From the passive and semi-active suspension designs (of quarter-car model) shown in Figure 1, we derive equations of motion of the two mass bodies which are un-sprung mass (half of axle mass and one wheel) m_u and sprung mass (quarter car body mass) m_s. The equations of motion of the systems (Figure 1.a and 1.b) are

a Passive suspension system:

$$\begin{cases} m_s\ddot{z}_s + c_s(\dot{z}_s - \dot{z}_u) + k_s(z_s - z_u) = 0 \\ m_u\ddot{z}_u + c_s(\dot{z}_u - \dot{z}_s) + k_s(z_u - z_s) + c_u\dot{z}_u + k_u z_u = k_u r + c_u\dot{r} \end{cases} \quad (1)$$

b Semi-active suspension system:

$$\begin{cases} m_s\ddot{z}_s + c_s(\dot{z}_s - \dot{z}_u) + k_s(z_s - z_u) = U_c \\ m_u\ddot{z}_u + c_s(\dot{z}_u - \dot{z}_s) + k_s(z_u - z_s) + c_u\dot{z}_u + k_u z_u = -U_c + k_u r + c_u\dot{r} \end{cases} \quad (2)$$

Where $z_s, \dot{z}_s$ and $\ddot{z}_s$ are displacement, velocity and acceleration of the sprung mass (quarter car body mass), respectively; $z_u, \dot{z}_u$ and $\ddot{z}_u$ are displacement, velocity and acceleration of the un-sprung mass (half of axle mass and one wheel), respectively; c_s and c_u damping coefficients of suspension and tire; k_s and k_u stiffness of suspension and tire; $r(t)$ and $\dot{r}$ are terrain roughness (disturbance) displacement and velocity with respect to longitudinal speed of the vehicle; U_c is the force generated by the controller that takes into account terrain irregularities $r(t)$, that is the vertical displacement, the function of time and dependent of the vehicle speed. In the model (2), U_c is the control force exerted by the controller. Our objective is to design such a controllable damper, capable of generating such control force

U_c that responds to profile irregularities adequately by providing comfort ride. For the controller model of the damper, we apply different hysteresis effect models, such as, Bingham, Dahl, LuGre and Bouc-Wen models and design numerical simulation models in MATLAB/Simulink. Mathematical formulations and simulation models of these four models are expressed in the following section with respect to a vehicle suspension system.

3. Mathematical Formulations and Simulation Models of the MR Dampers

3.1. Bingham Model

Dynamic hysteresis behaviors of the MR liquid dampers are expressed by several different mathematical formulations. One of the simplest ones is the Bingham model [9]. The Bingham plastic model [9] for the physical model shown in Figure 2 is formulated by the following first order differential equation:

$$F_{mr} = F_c\, sgn(\dot{z}) + c_0\dot{z} + K_0 z + F_0 \tag{3}$$

Where z is relative displacement of a piston that corresponds to the displacement (z_s) of a suspended mass (m_s) and $\dot{z}$ is its derivative that is velocity of a piston; F_c is frictional (control) force; c_0 is damping constant; K_0 is stiffness of an elastic element of the damper; F_0 is offset force (constant force value). The signum function $sgn(\dot{z})$ will take care of the direction of the frictional force F_c with respect to the relative velocity $\dot{z}$ of the hysteresis (internal) variable z. Note that in the simulation model, z and velocity $\dot{z}$ correspond to the displacement z_s and velocity $\dot{z}_s$ of the sprung (suspended) mass m_s (quarter car body mass) (see Figure 1). It should be noted that besides this model given in (3), there are several other alternative formulations of the Bingham model, for instance, the Bingham visco-plastic model.

The Bingham model takes into account the Coulomb (dry) friction, plain (constant) damping, stiffness and some constant offset force and its control force direction changes with respect to the value of the sprung mass velocity $\dot{z}_s$. Thus, its controllable damping force F_c contributes in intensity of damping or releasing damping force in order to provide fast and efficient damping of potential and kinetic energy induced by the road profile roughness.

Even though the expression in (3) is a plain formulation, but it is not straightforward to use it in numerical simulations because of discontinuity of the signum function $sgn(\,)$. Therefore, there is an alternative formulation to express the signum function approximately by the inverse tangent function.

$$F_{mr} = \frac{2F_c \tan^{-1}(d\cdot\dot{z})}{\pi} + c_0\dot{z} + K_0 z + F_0 \tag{4}$$

Where a new term d, introduced in (4), is a form factor.

The response of Bingham model can be approximated as a graph shown in Figure 3 and can be assumed that the shape of the Bingham model force F_{mr} will be equal to Coulomb force plus friction force (F_c). The damping coefficient (constant) c_0 will be equal to the linear relationship between the force ΔF and the velocity $\Delta\dot{z}$ differences (see Figure 3).

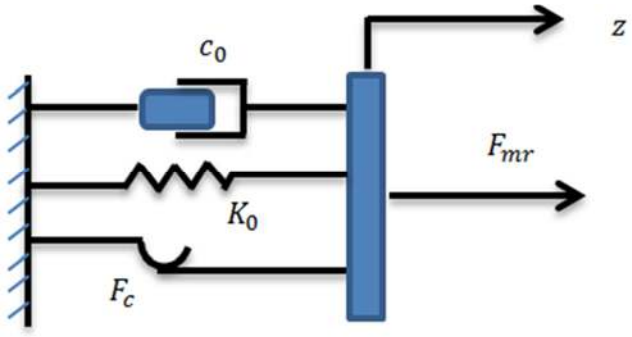

Figure 2. *Bingham mechanical model proposed by [17].*

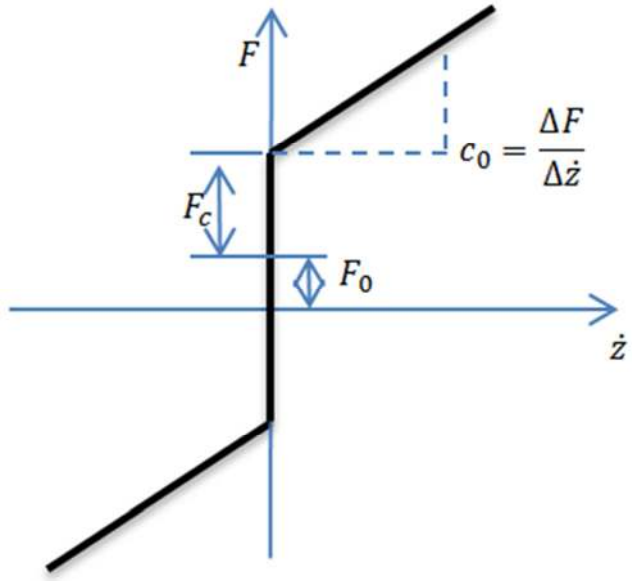

Figure 3. *The response of Bingham model.*

Note that in the Bingham model (Figure 3), the Coulomb frictional element is in parallel with a viscous dashpot – damper, and the Coulomb force (F_c) is directly related to the yield stress. The response of the Bingham model shown in Figure 3 is a rough approximation of the hysteresis loop expressed by the formulations given in (3) and (4), and the form factor d improves approximation of the hysteresis loops of (3) and (4) considerably.

Now we build a Simulink model – Figure 4 using the formulation from the equation (4) and link it with the model expressed for the semi-actively controlled suspension model from the expression of (2) as shown in Figure 1. b. In the Bingham model, F_{mr} active force of the damper is equal to a control force U_c in the semi-active suspension model – Figure 1, b and the above formulation (2). The Bingham model with two input signals, viz. displacement $z(t)$ and velocity $\dot{z}(t)$ of a quarter car body mass, and one output signal that is damping force exerted by the magneto-rheological damper F_{mr}, built in Simulink is shown in rectangle – Figure 4. The output signal (F_{mr}) goes to the sprung mass' summing junction with (-) sign and to the un-sprung mass' summing junction with (+) sign.

It is to be noted that the active control force U_c in the Bingham model is generated with respect to the feedback signal coming from the velocity ($\dot{z}_s(t)$) of the suspended (sprung) mass m_s.

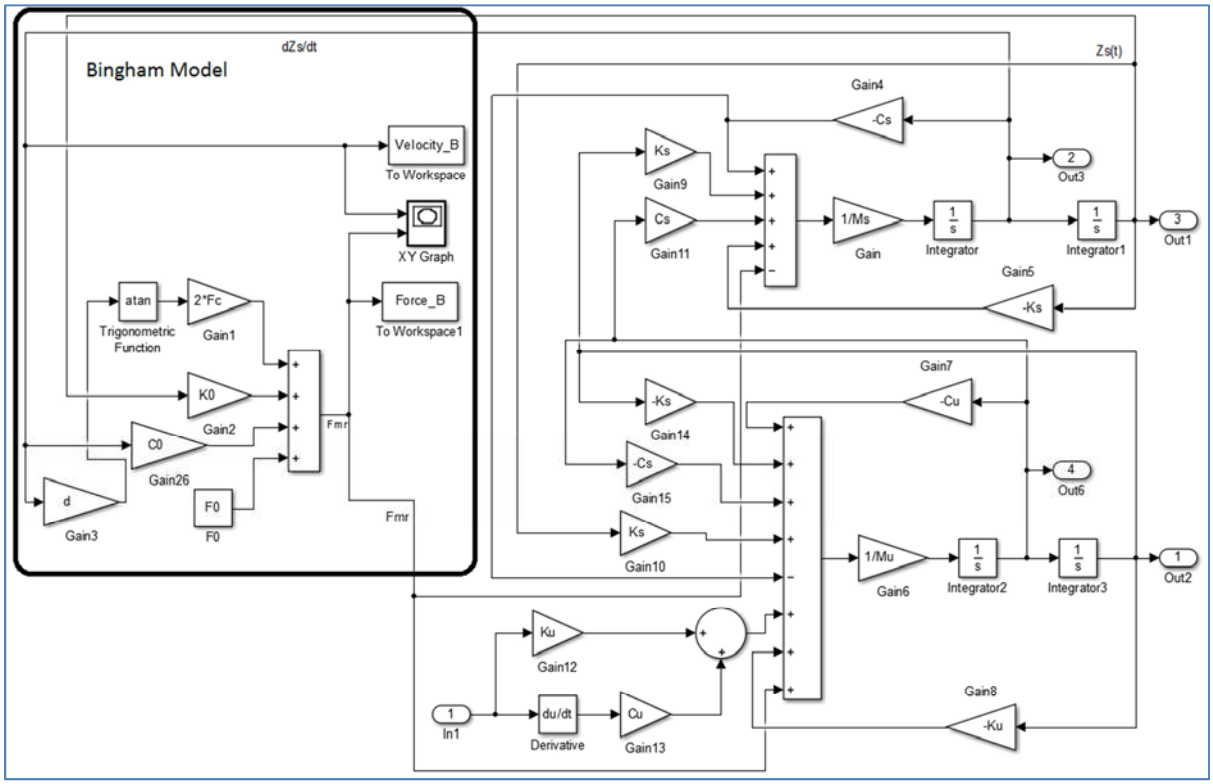

Figure 4. *Bingham model embedded in semi-active suspension model.*

3.2. Dahl Model

The Dahl model of the MR damper is formulated by [10] and in the modified version [17] of the model considers quasi-static bonds in the origin of friction. The Dahl model [10] is formulated by the following expressions:

$$F_{mr} = k\dot{z} + (k_{wa} + k_{wb}u)w \quad (5)$$

$$\dot{w} = \rho(\dot{z} - |\dot{z}|w) \quad (6)$$

Where, F_{mr} is exerted force from the MR damper, u is the control voltage, w is the dynamic hysteresis coefficient, k, k_{wa}, k_{wb} and ρ are parameters that control the hysteresis loop shape. Using the expressions (5) and (6), we build a simulation model of Dahl model in Simulink as shown in Figure 5. In the Simulink model (Figure 5), there is one feedback coming that is velocity $\dot{z}$ $(dz_s(t)/dt)$ of the sprung mass m_s. The exerted force F_{mr} of the MR damper corresponds to the control force U_c shown in Figure 1.

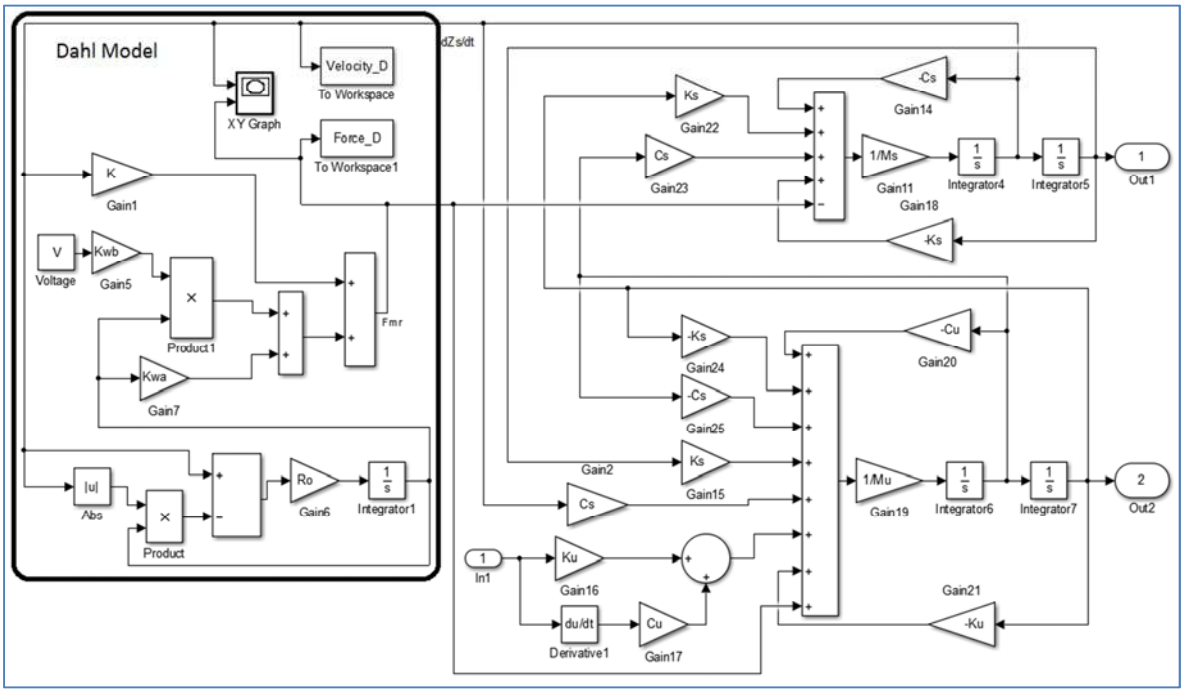

Figure 5. *Dahl model implemented in semi-active suspension model.*

In the Dahl model alike the Bingham model, the feedback (input) signal dz_s/dt is coming from the velocity ($\dot{z}_s$) of the sprung mass that is a car body velocity and feeding the summing junction of F_{mr} force, and summing junction of w dynamic hysteresis coefficient. The output signal is the control force F_{mr} feeding a summing junction of input forces for sprung mass with (-) sign and un-sprung mass with (+) sign.

It should be noted that in the Dahl model, the generated control force (or damping force) considers the difference in-between actual and absolute values of the sprung (suspended) mass velocity ($\dot{z}_s$). There are several factors by which dynamic hysteresis behavior can be formulated with the Dahl model better than with the Bingham model. But how this improved formulation influences on the performances of the Dahl model with respect to the Bingham model will be studied in our numerical simulations.

3.3. LuGre Model

In modeling the hysteresis loops, the LuGre model is developed within studies [11, 12] and applied in works [18, 19] in modeling and simulation of dampers. The model given in [12] takes into account three types of frictions observed in dry friction and fluid flows, viz. Coulomb, stick-slip and stribeck effects that are formulated by the following expression:

$$F_{mr}(t) = \sigma_0 y(t) + \sigma_1 \dot{y}(t) + \sigma_2 \dot{z}(t) \tag{7}$$

Where $\sigma_0, \sigma_1, \sigma_2$ are stiffness, damping and viscous friction coefficients, respectively; $y(t)$ is the friction state (average deflection of the bristles), $\dot{y}(t)$ is the velocity of the friction state, $\dot{z}(t)$ is the relative velocity of the sprung mass.

$$\dot{y}(t) = \dot{z}(t) - \frac{|\dot{z}(t)|}{y_{ss}(\dot{z}(t))} y(t) \tag{8}$$

In the above expression, $y_{ss}(\dot{z}(t))$ is defined by [11 and 18] that has been expressed with the following

$$y_{ss}(\dot{z}(t)) = \frac{1}{\sigma_0}\left(F_c + (F_s - F_c)e^{-\left(\frac{\dot{z}(t)}{v_s}\right)^2}\right) \tag{9}$$

Where F_c is the Coulomb friction force, F_s is the sticktion force, and v_s is the Stribeck velocity.

The simulation model of the LuGre model, as shown in Figure 6, is built in Simulink with one input signal that is a relative velocity from the sprung mass and one output signal that is control force F_{mr} going to summation junctions of the sprung and un-sprung masses with (-) and (+) signs respectively alike the Bingham and Dahl models shown in Figure 4 and 5.

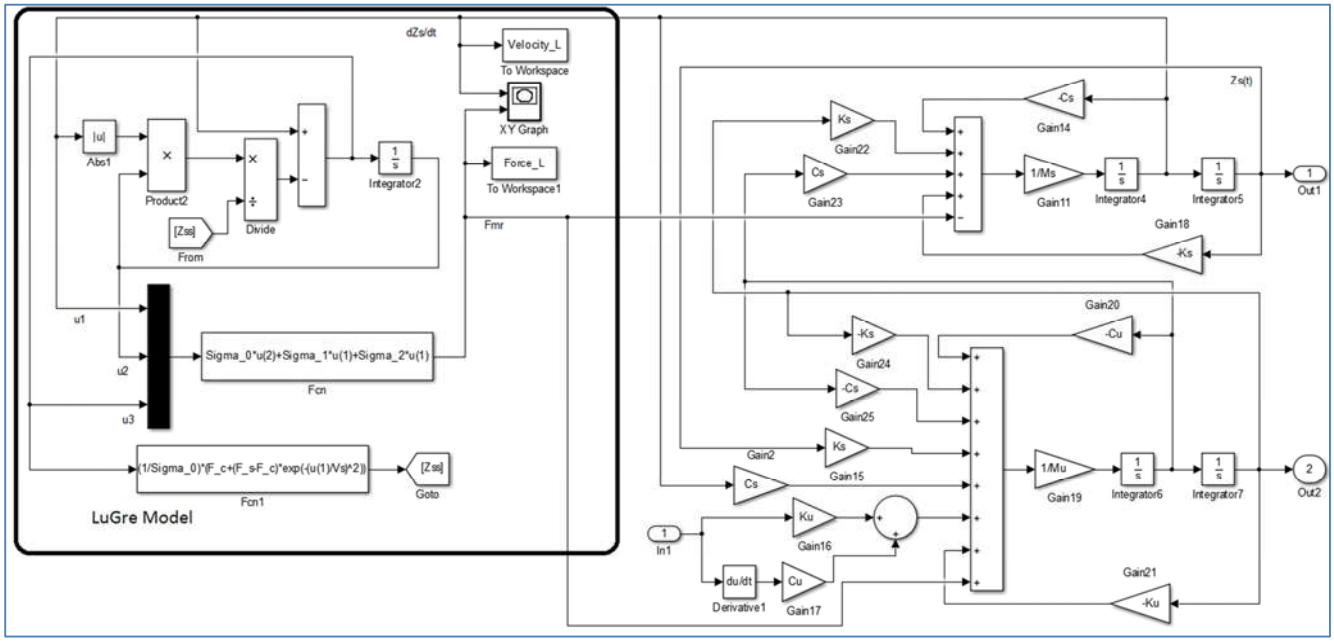

Figure 6. *The LuGre model implemented in semi-active suspension model.*

In the Simulink model, a function block with three input signals, viz. $\dot{z}(t), y(t), \dot{y}(t)$, is employed to compute a control force that is the MR force F_{mr}. The two input signals, which are $y(t)$ and $\dot{y}(t)$, are internal variables computed from the expressions (8) and (9). The LuGre model expression considers the Coulomb, stick-slip and stribeck effects observed in the non-Newtonian liquids. In this regard, this model expresses the dynamic hysteresis behavior of the MR dampers better than the two previous models.

3.4. Bouc-Wen Model

The MR damper with the Bouc-Wen model is composed of stiffness (spring) element, passive damper and Bouc-Wen hysteresis loop elements. The schematic representation of the Bouc-Wen model of the MR damper is depicted by the next schematic view – Figure 7. The hysteresis loop has an internal variable y that represents hysteretic behavior and satisfies the next expression (10). The model equation of the Bouc-Wen model [13, 14] is expressed by the following.

$$\dot{y} = -\gamma|\dot{z}|\, y\, |y|^{n-1} - \beta z\, |y|^n + A\dot{z} \tag{10}$$

Where y is the evolutionary variable that can vary from a sinusoidal to a quasi-rectangular function of the time depending on the parameters γ, β and A.

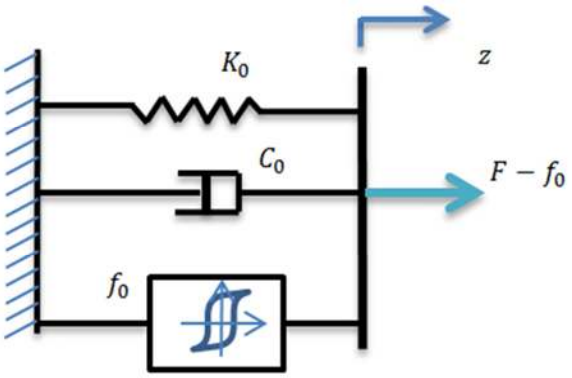

Figure 7. *Schematic representation of the Bouc-Wen model [15] of the MR damper.*

The force exerted by the MR damper is the function of the relative displacement z and velocity $\dot{z}$, and the parameter α defined by the control voltage u and is given by

$$F_{mr} = C_0(u)\dot{z} + K_0 z + \alpha(u)y + f_0 \qquad (11)$$

In the model, K_0 is the stiffness of the spring element of the MR damper and the values of the parameters (coefficients) $C_0(u)$ and $\alpha(u)$ have a linear relationship with the control voltage u and determine the influence of the model on the final force F_{mr}. The force f_0 takes into account pre-yield stress of the damper. The values of the parameters (coefficients) $C_0(u)$ and $\alpha(u)$ are determined from the following expressions:

$$C_0(u) = C_{0a} + C_{0b}u, \alpha(u) = \alpha_{0a} + \alpha_{0b}u \qquad (12)$$

The best-fit parameter values of these parameters are determined by fitting to the experimentally measured response of the system. Also, for parameter identification of the MR dampers, different reference signals are used, i.e. T-wave periodic signals [20] are used to define parameters in the Dahl and Bouc-Wen models. It should be noted that in our simulations, we take constant values for C_0 and α.

The simulation model of the system from the Bouc-Wen model shown in Figure 8 is built in Simulink by using the equations expressed in (10) and (11). The simulation model has two input sources, viz. $z(t)$ displacement and $dz(t)$ velocity of the sprung mass (m_s) of the system, and two output signals for control force F_{mr} going to the sprung mass (m_s) with (-) minus sign and to the un-sprung (m_u) mass with (+) plus sign. Note that $dz(t)$ is equal to $\dot{z}(t)$ and F_{mr} is equal to U_c in the equation (2). Note that in the Bouc-Wen model, there are two input signals and one output signal. The input signals are $z(t)$ and $\dot{z}(t)$ displacement and velocity of the sprung mass and the output signal is the control force F_{mr} generated by the MR damper.

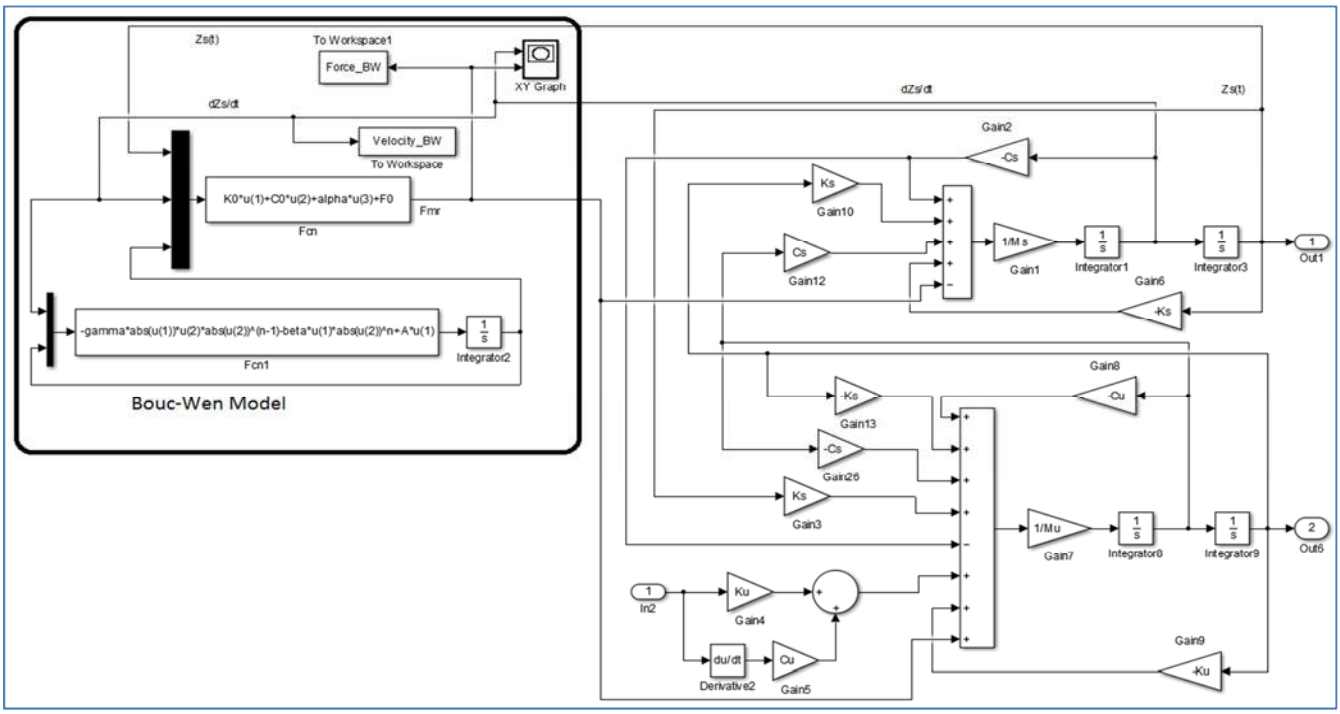

Figure 8. *Bouc-Wen model implemented in semi-active suspension.*

In the Bouc-Wen model alike the Bingham, Dahl and LuGre models, the control force feeds the summing junction of forces for the sprung mass with (-) sign and the un-sprung mass with (+) sign.

The Bouc-Wen model's representation given in Figure 7 is similar to the Bingham model given Figure 2, but there are considerably improved formulation of dynamic hysteresis behaviors of the MR liquids with the evolutionary variable y. Even though the formulations of the Bouc-Wen model are rather complicated in comparison with the other three models, but it gives much better expression and control over dynamic hysteresis behavior of the non-Newtonian liquids like the MR liquids than the other three models.

All of the four simulation models are made up as sub-systems (Figure 9) to compare their performances against each other and a passively controlled system for four different excitation signals from the terrain. The system response is $z(t)$ displacement of the car body (sprung mass) from the road excitations. Road profile irregularities $r(t)$ are generated numerically by the Heaviside step function (13), white noise generated by uniform random

number, sine waves, and sum of sine waves and white Gaussian noise with 2.5 dBW power (14). All of the excitation signals are set to have maximum magnitude of 0.075 m.

The Heaviside step function $r(t)$ representing road irregularities is defined to be:

$$r(t) = \begin{cases} 0 \; t < 1 \\ 0.75 \; t = 1 \\ 0.75 \; t > 1 \end{cases} \quad (13)$$

Sum of pure sine and white Gaussian noise:

$$r(t) = A * \sin(2\pi f t) + GWN \; (with \; 2.5 \; dBW \; power) \quad (14)$$

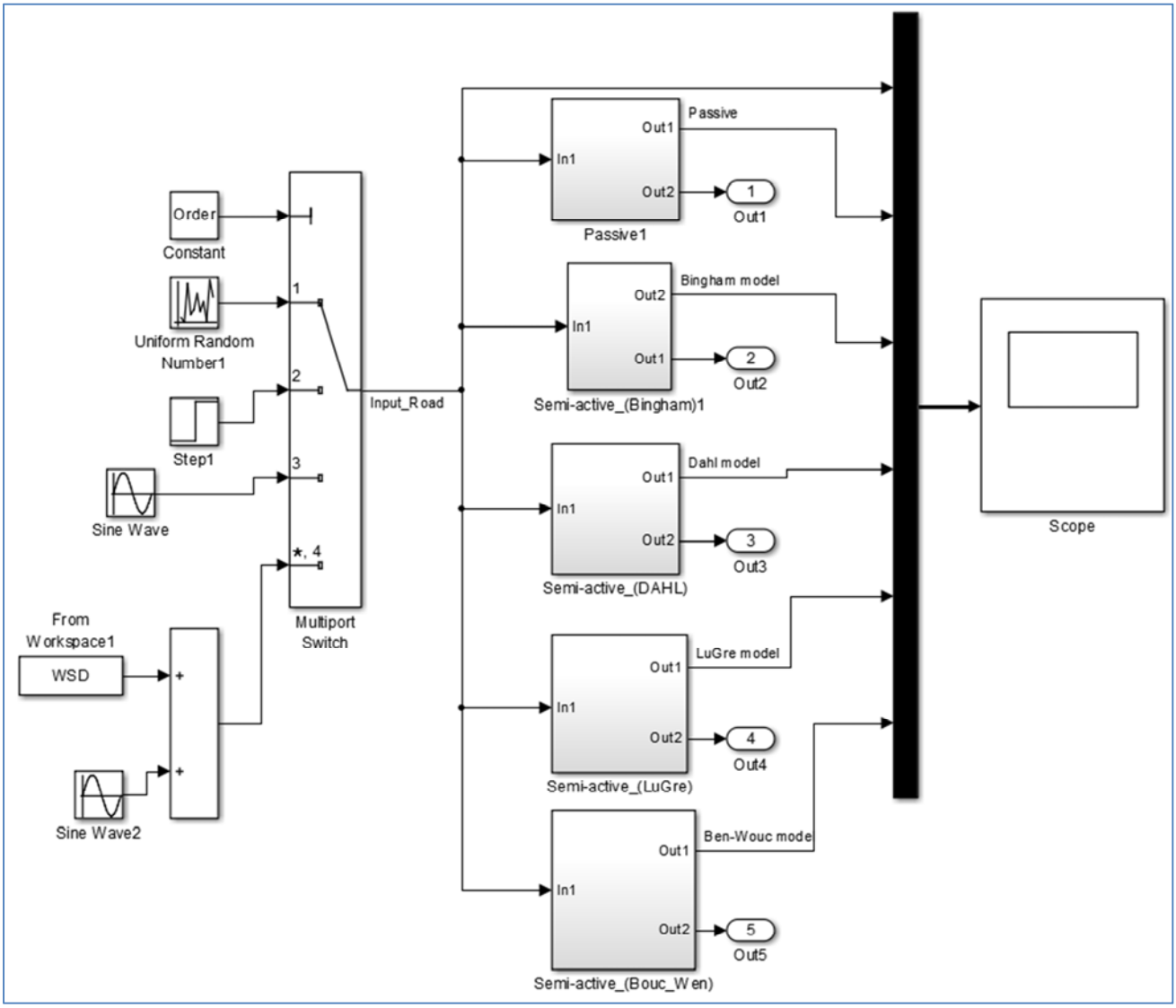

Figure 9. *Passively controlled system model vs. four MR models as sub-systems.*

All of the four models of the MR liquid dampers express hysteresis behaviors of the non-Newtonian liquids used in dampers or shock absorbers. These models differ in their efficiency and formulations of the dynamic hysteresis loops, and have some advantages and drawbacks in study processes and applications. That we discuss in our comparative analyses of these models' performances in the following section.

4. Simulation Results and Discussions

The above depicted mathematical formulations of the MR models implemented in Simulink models are simulated and compared their performances to analyze generated damping force, and vibration and shock damping efficiency as a semi-active vibration controller from the system equations (2) of motion against passively controlled/damped vibration damper formulated in (1) in the example of quarter car model shown in Figure 1. In all of our simulations, the control force U_c is set to be equal to F_{mr} and a damped vibration level on the sprung mass is evaluated. Displacement of the sprung mass is considered. The values of suspension parameters (quarter car) are taken from the Golden Car model [21, 22] parameters given in Table 1. It should be noted that the Golden Car parameters are recommended [23] in studies for assessment of comfort ride and road roughness index. Damping of a tire is not taken into consideration in the Golden Car model and thus, we set its value equal to zero. All numerical values for hysteresis model (Bingham, Dahl, LuGre and Bouc-Wen) parameters are given in Table 2, 3, 4 and 5. The rational parameter values of the hysteresis models (given in bold in Table 2, 3, 4 and 5) are found by trails and

errors. For numerical simulations, four different signals, viz. random white noise generated with uniform random number generator within a range of -0.0375 and 0.0375 m, Heaviside step function with the magnitude of 0.075 m, sine waves with 7.77 rad/sec and 67.3 rad/sec of oscillations and combinatorial excitation signal, that is a sum of sine waves with 7.77 rad/sec and 67.3 rad/sec of oscillations and Gaussian noises with the power of 2.5dBW, are taken. Oscillation frequencies of sine waves are taken by considering natural frequencies of the quarter car model with the Golden Car parameters or in other words, poles of the system's transfer function.

Table 1. *Data for a quarter car model – Golden car parameters [20, 21].*

Parameter name	Parameter notation	Parameter value
Sprung Mass	m_s	450 $[kg]$
Un-sprung Mass	m_u	68 $[kg]$
Stiffness of Suspension	k_s	28500 $[N/m]$
Stiffness of Un-spring Mass (tire)	k_u	293900 $[N/m]$
Damping Coefficient of Sprung Mass	c_s	2700 $[N \cdot s/m]$
Damping Coefficient of Un-sprung Mass	c_u	0 $[N \cdot s/m]$
Normalized Sprung Mass	m_s/m_s	1
Normalized Un-sprung Mass	m_u/m_s	0.15
Normalized Stiffness of Suspension	k_s/m_s	63.3 $[1/s^2]$
Normalized Stiffness of Un-sprung Mass	k_u/m_s	653 $[1/s^2]$
Normalized Damping of Sprung Mass	c_s/m_s	6 $[1/s]$

Table 2. *Data for the Bingham model simulation.*

Parameter name	Parameter notation	Parameter value
Damping coefficient in Bingham model	c_0	650 $[N \cdot s/m]$
Offset force	F_0	0 $[N]$
Frictional force	F_c	210 $[N]$
Stiffness of an elastic component	k_0	300 $[N/m]$
Form factor	d	[5, 10, 20, 30, 60]

Table 3. *Data for the Dahl model simulation.*

Parameter name	Parameter notation	Parameter value
Control voltage	u	[0.75, 1.5, 3, 5] $[V]$
Hysteresis parameters	k, k_{wa}, k_{wb}, ρ	[2; 40; 40; 750], [5; 80; 80; 1500], [10; 160; 160; 3000], [5; 80; 80; 1500]

Table 4. *Data for the LuGre model simulation.*

Parameter name	Parameter notation	Parameter value
Coulomb friction force	F_c	210 $[N]$
Sticktion force	F_s	150 $[N]$
Stribeck velocity	v_s	5 $[m/s]$
Stiffness coefficient	σ_0	$[5 * 10^4; \mathbf{10^5}; 2 * 10^5; 3{*}10^5]$ $[N/m]$
Damping coefficient	σ_1	$[0.5 * \sqrt{10^4}; \sqrt{\mathbf{10^4}}; 2\sqrt{10^4}; 3\sqrt{10^4}]$ $\left[N \cdot \frac{s}{m}\right]$
Viscous friction coefficient	σ_2	[0.2; 0.4; 0.8; 1.2] $[N \cdot s/m]$

Table 5. *Data for the Bouc-Wen model simulation.*

Parameter name	Parameter notation	Parameter value
Parameters of the Hysteresis shape	γ, β, A, n	$[0.6 * 10^6, 5 * 10^5, 7.5, 1]$, $[\mathbf{1.2 * 10^6, 10^6, 15, 2}]$, $[2.4 * 10^6, 2 * 10^6, 30, 4]$, $[3.6 * 10^6, 3 * 10^6, 45, 6]$
Stiffness of the spring element	K_0	300 $[N/m]$
Damping coefficient	C_0	650 $[Ns/m]$
Input voltage u	u	5 $[V]$
Other parameters	α	80000
Pre-yield stress	f_0	0 $[N]$

One of the very first conclusion from the simulations is that the hysteresis loop models with the Bingham, Dahl, LuGre and Bouc-Wen models for the semi-active suspension system outperform a passive suspension system model for our four considered excitation signals $r(t)$ from the road profile. For instance, Figure 10 and 11 demonstrate system responses (displacement of the car body that is the suspended mass m_s) of the passively and semi-actively controlled models on random white noise (generated by the uniform number) within amplitude of -0.0375 m and +0.0375 m. In this case, all hysteresis models outperform passively damped system model in damping undesired excitations from the terrain in terms of their responsiveness and efficiency.

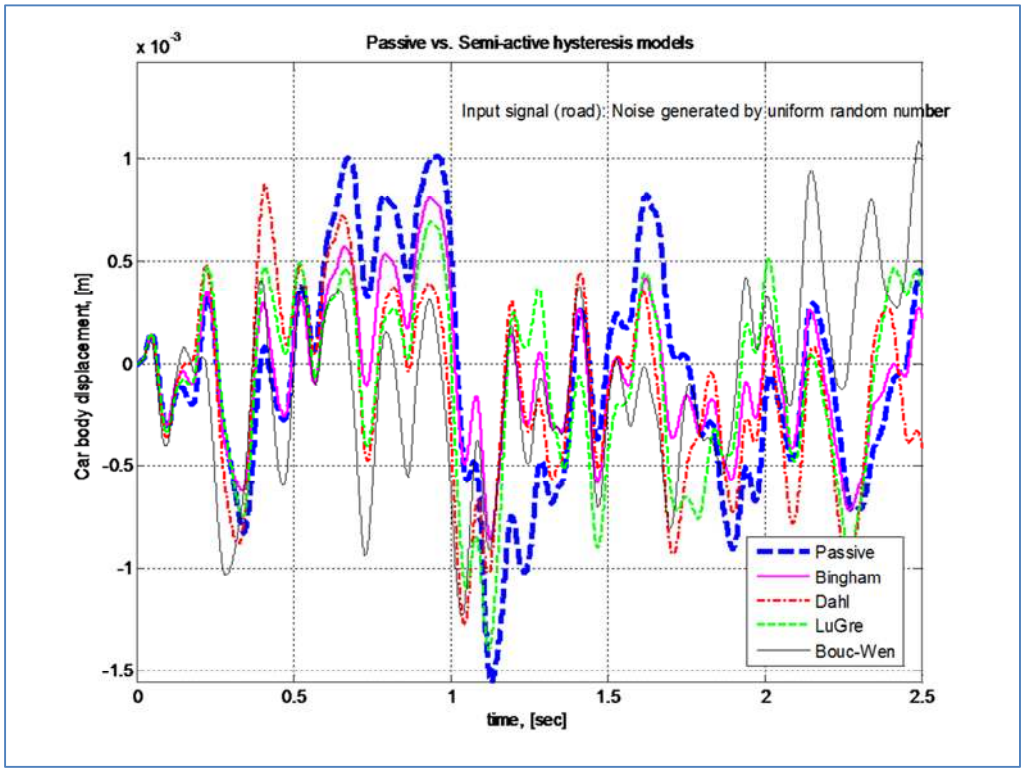

Figure 10. *Model responses on random noise excitation from road.*

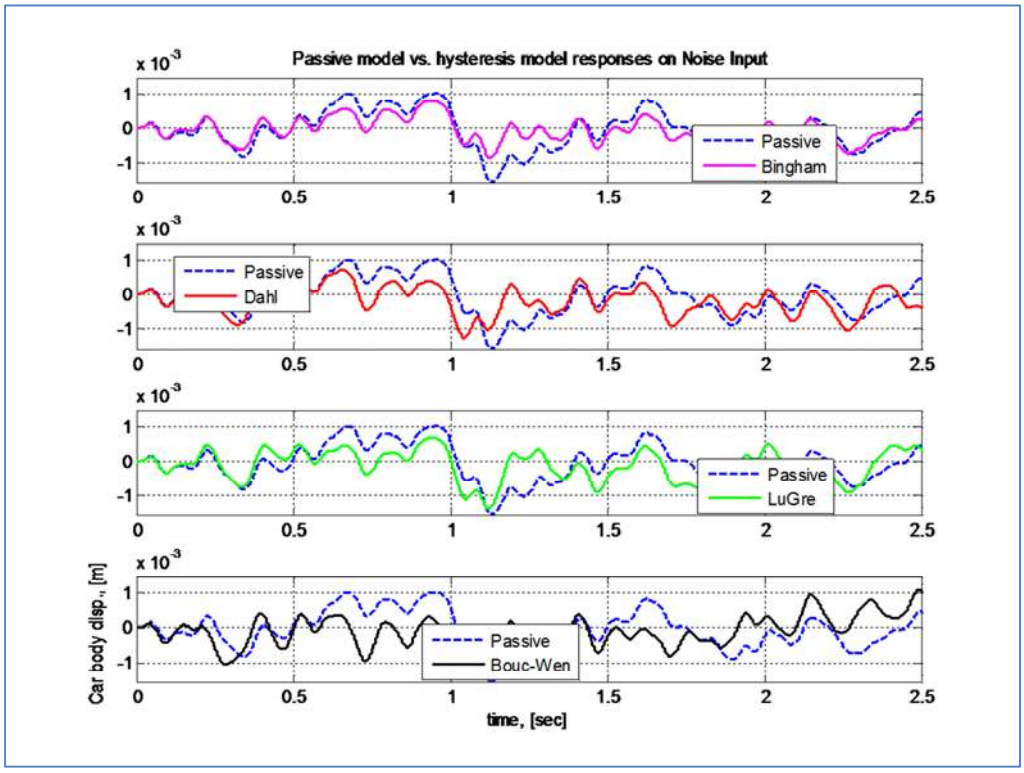

Figure 11. *Model responses on random noise excitation from road.*

In another simulation with Step (Heaviside) function expressed by the formulation of (13) with the magnitude of 0.075 m shown in Figure 12 and 13, the hysteresis models have outperformed in damping undesired excitation in the car body in comparison with passively controlled system model. In this case, the MR damper models have reached to steady state value in less than one second whereas a passive suspension model has reached to the steady state after two seconds. On the other hand, the Bouc-Wen model has kept some very low amplitude and higher frequency fluctuations for a few seconds after steady state. Again, responses of the four MR damper models are similarly fast, but Bingham model has outperformed the other three models in terms of damped excitation magnitude and speed of responsiveness.

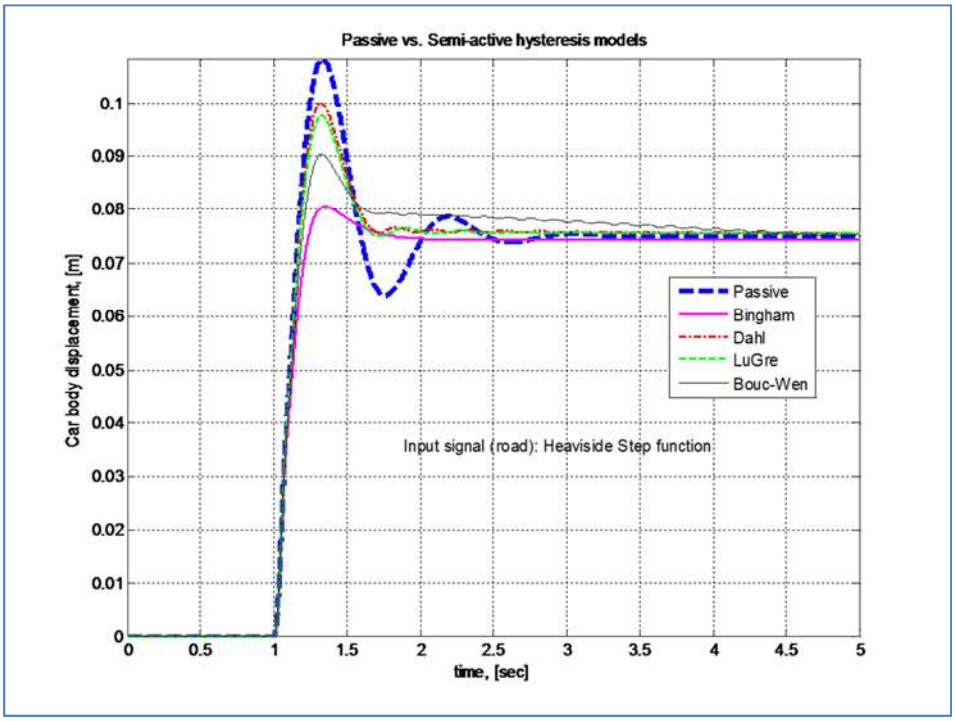

Figure 12. *Passive vs. Semi-active suspension models on step input excitation.*

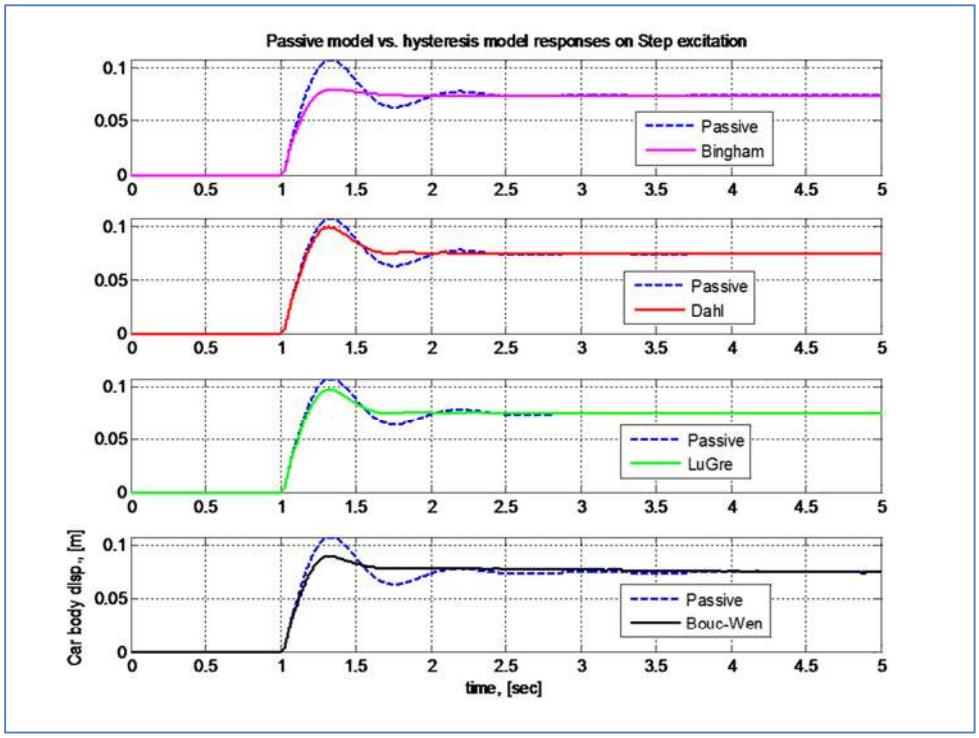

Figure 13. *Step response of the passive and semi-active suspension models.*

Figure 14 shows the system responses with the Bingham and Bouc-Wen models on random noise input (from road profile) generated by the uniform random number function (block) of MATLAB®/Simulink®. The performances of the two hysteresis models show that undesired vibration damping is considerable in comparison with the passive suspension model. The hysteresis loop plots shown in Figure 15 – 18 demonstrate generated MR damping force vs. velocity of a sprung mass (equal to velocity of a damper's piston). From the plots of velocity vs. the force generated by the Bingham model (Figure 15) and LuGre model (Figure 17) for a sine wave input with a frequency of 7.77 rad/sec, the magnitude of the generated force magnitude is two times higher with the Bingham model than with the LuGre model. Similarly, in the Bouc-Wen model (Figure 18), the generated force magnitude is twice higher than the force magnitude generated by the Dahl model (Figure 16) when sine wave signals with 67.3 rad/sec frequencies are applied as an input signal. In all models hysteresis loops are preserved but their yield stresses have differed.

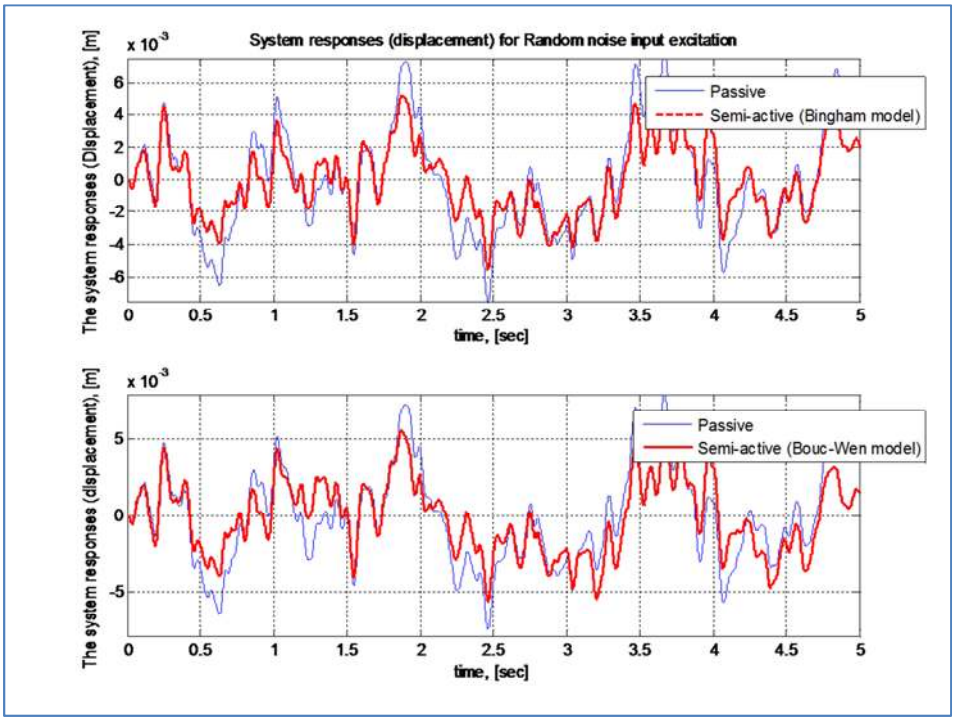

Figure 14. *System responses on random noise excitation.*

In sine wave excitations with 7.77 rad/sec of frequency shown in Figure 15 and 16, all hysteresis models have performed considerably better in damping oscillations in the sprung mass in comparison with the passive suspension model. At the same time, the Bingham model has outperformed all other models, viz. Dahl, LuGre and Bouc-Wen in terms of damped vibration magnitude levels. However, periodic oscillations have remained with all models. The performances of all models (Figure 17) for higher frequency oscillations with 67.3 rad/sec (exerted from an input signal) of sine waves have been very close to the passive suspension model performance and thus, they efficiency has been marginal in dissipating energy from this periodic excitation.

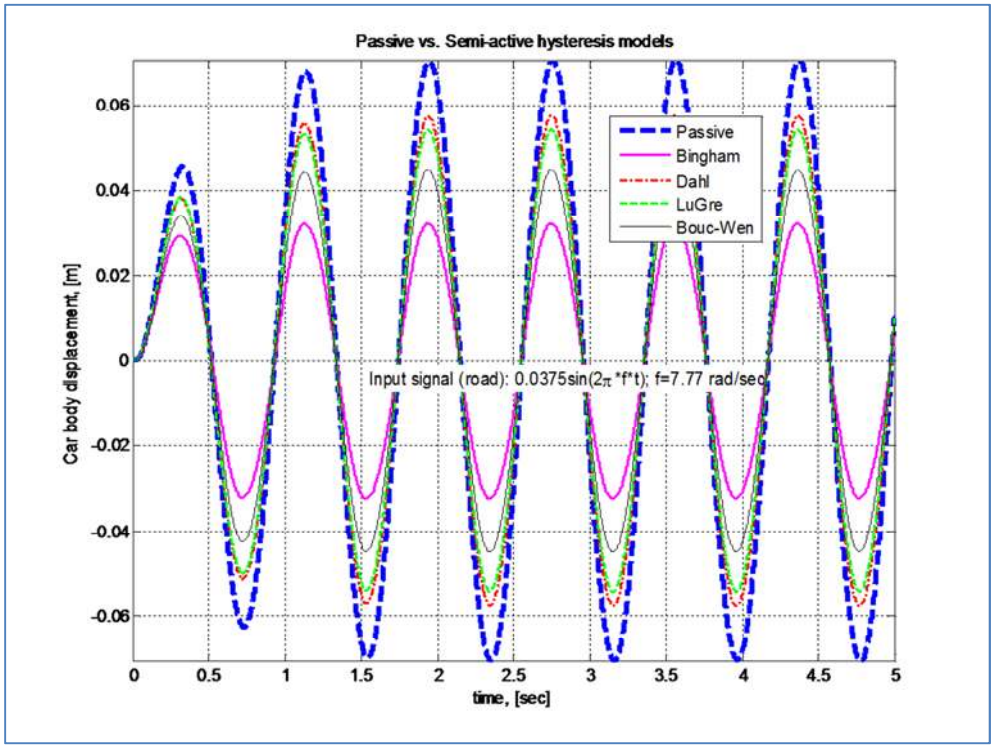

Figure 15. *Passive vs. Semi-active suspension performances on sinusoidal wave:* $0.0375\,sin(2\pi ft)$, f *=7.77 rad/sec excitation.*

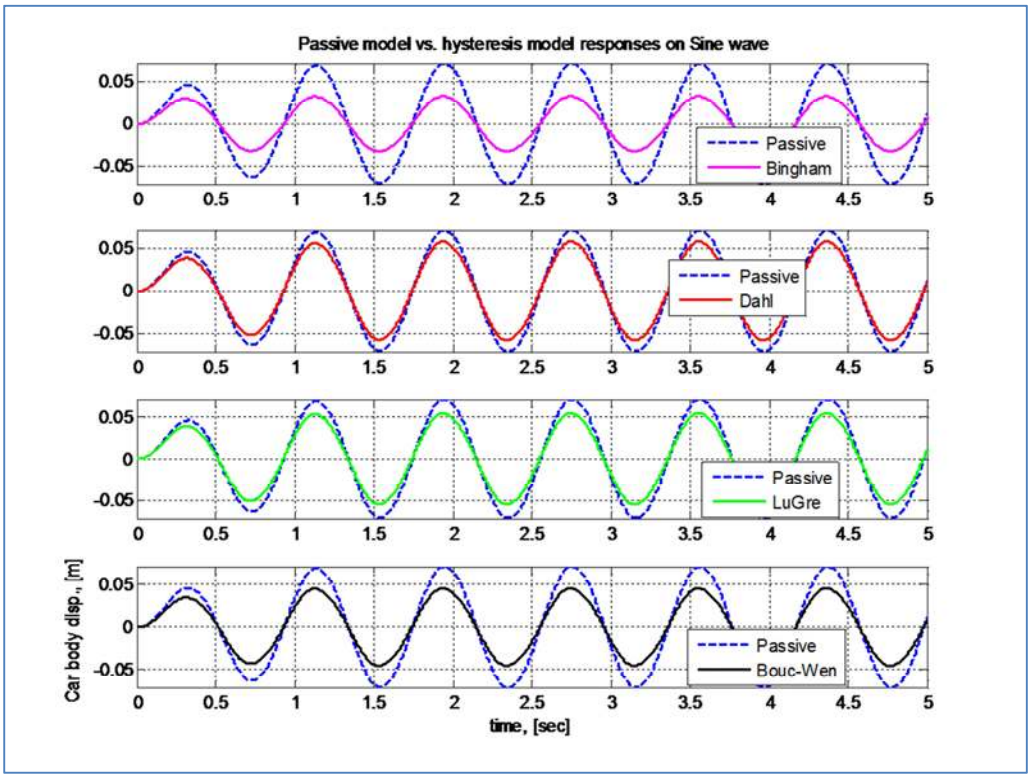

Figure 16. *Passive vs. Semi-active suspension performances on sine wave:* $0.0375\,sin(2\pi ft)$, $f = 7.77$ *rad/sec excitation.*

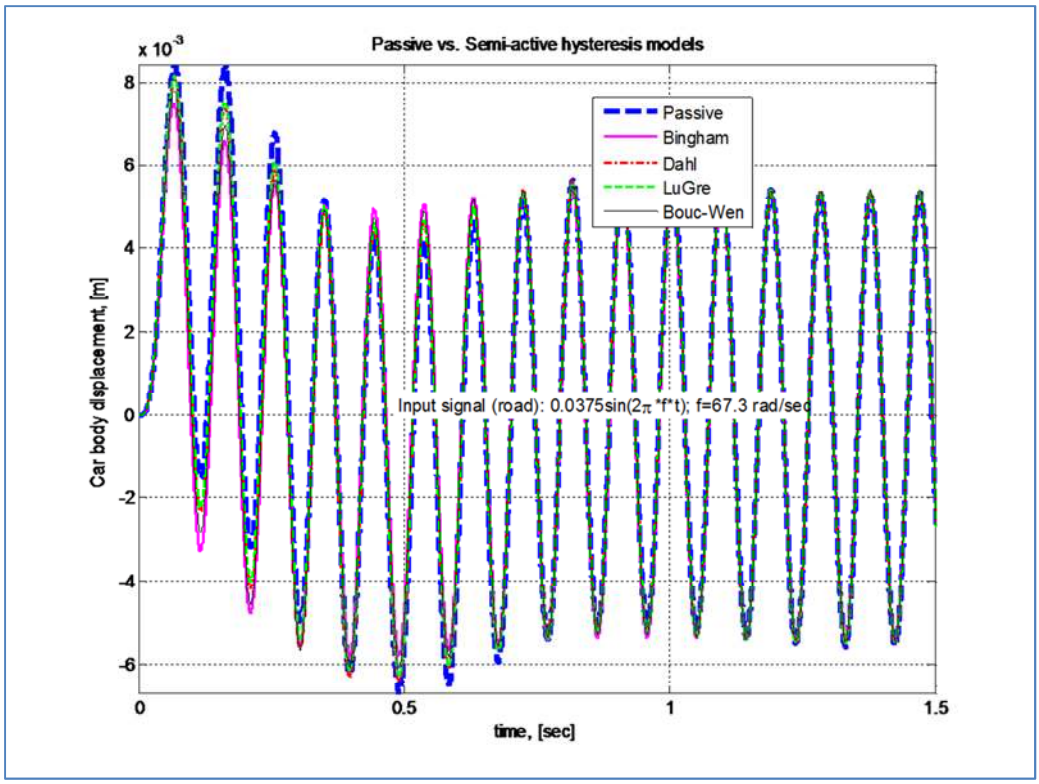

Figure 17. *Passive vs. Semi-active suspension responses on sine wave:* $0.075\,sin(2\pi ft)$, $f = 67.3$ *rad/sec excitation.*

A fourth excitation signal from road profile used to simulate the models is sine wave with 67.3 rad/sec of frequency plus white Gaussian noise expressed by the expression of (14). The performances of the semi-active models for this excitation – Figure 18 and 19 have been similar to the previous case and the efficiency of all MR models has been very marginal in comparison with the passive suspension model. From these simulations, we conclude that when there are high frequency excitations, efficiency of the MR dampers with our set parameter values (given in bold in Table 2, 3, 4, and 5) may not be high. Therefore, in order to study influence of the hysteresis loop parameters of the MR models, we have performed four and five separate simulations for each model with different parameter values.

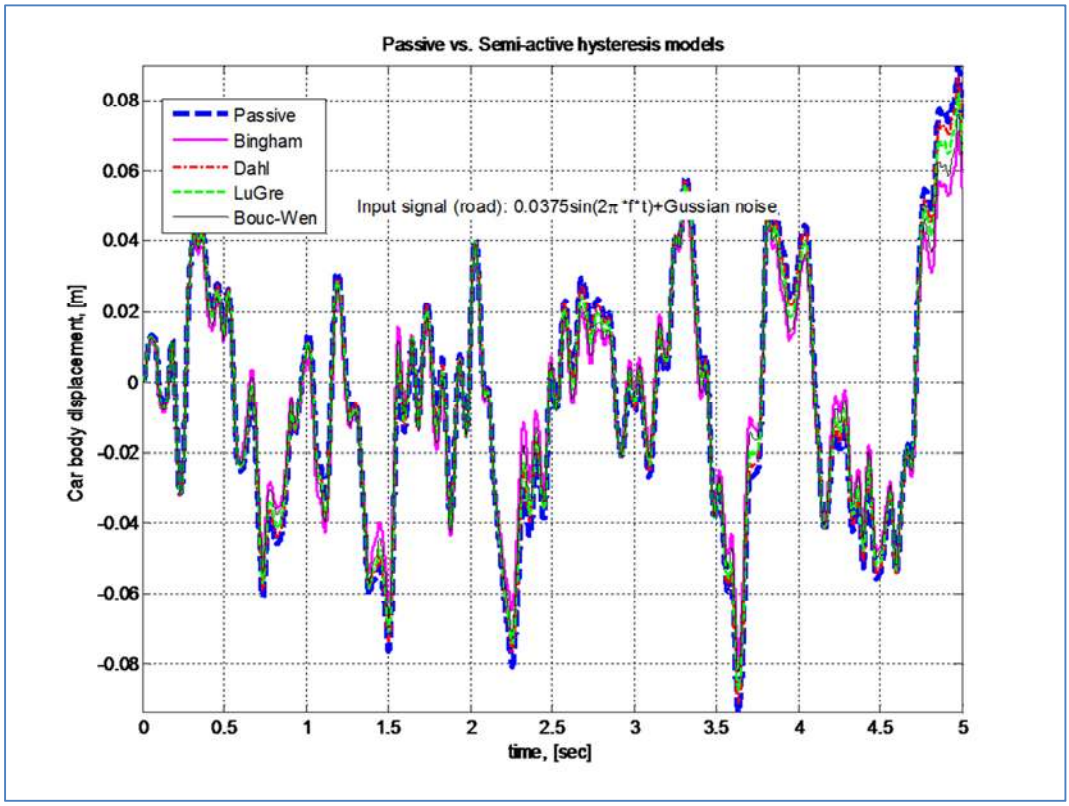

Figure 18. *The system responses of passive and semi-active on sine wave ($f = 67.3$ rad/sec):* $0.075\,sin(2\pi ft)$ *+ white Gaussian noise (with power of 2.5 dBW) excitation.*

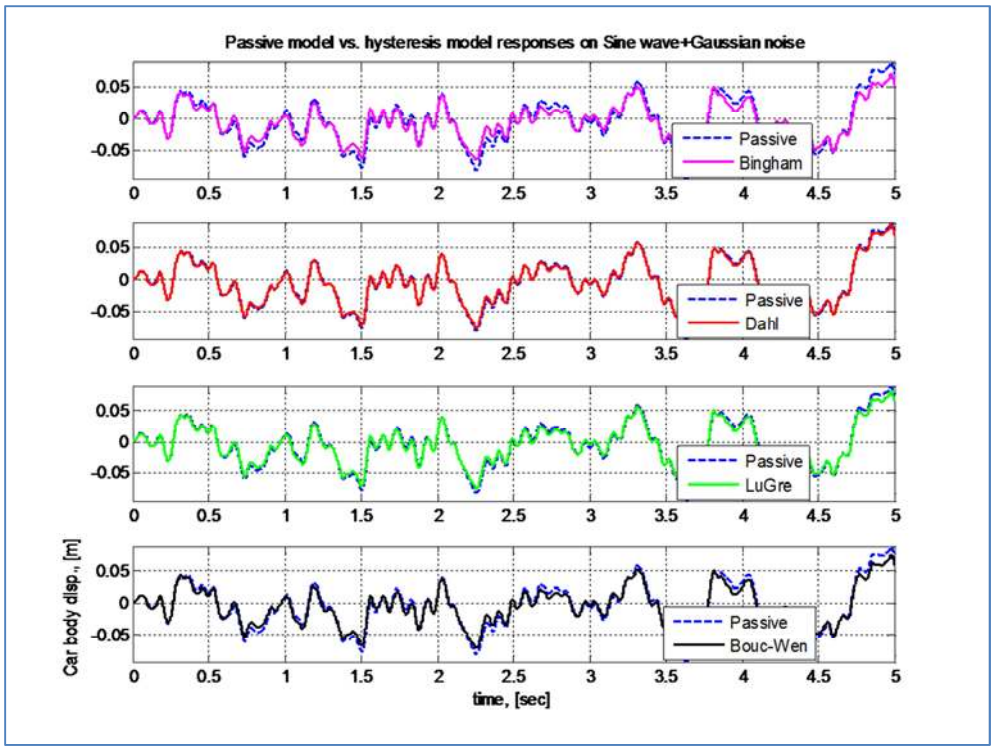

Figure 19. *The system responses of passive and semi-active on sine wave ($f = 67.3$ rad/sec):* $0.0375\,sin(2\pi ft)$ *+ white Gaussian noise (with power of 2.5 dBW) excitation.*

First, we have studied an effect of the form factor d on the performances of the Bingham model. Figure 20 and 21 show how the form factor d influences on the change of the dynamic hysteresis loop shape and damping for sine wave (with 7.77 rad/sec) excitation from the road profile. From these studies, we can conclude that by increasing the value of d the hysteresis form changes from approximately linear form into "S" type loop form. Also, by increasing the value of d, we can attain better performances in terms of damped vibration; however, the rate of increase in values of d reaches

to stagnation after its certain values, e.g. $d = 30$. The stagnation can be also observed in Figure 22 on the Heaviside step excitation expressed in (13).

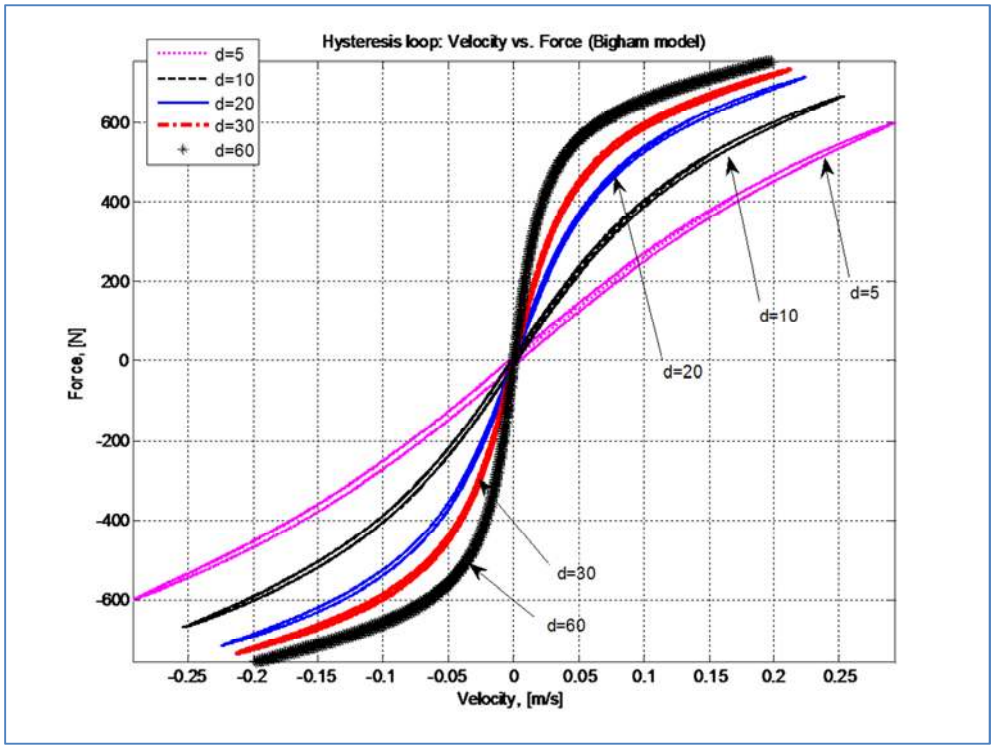

Figure 20. *Bingham model response on sine wave (with 7.77 rad/sec) excitation with different values of the form factor d.*

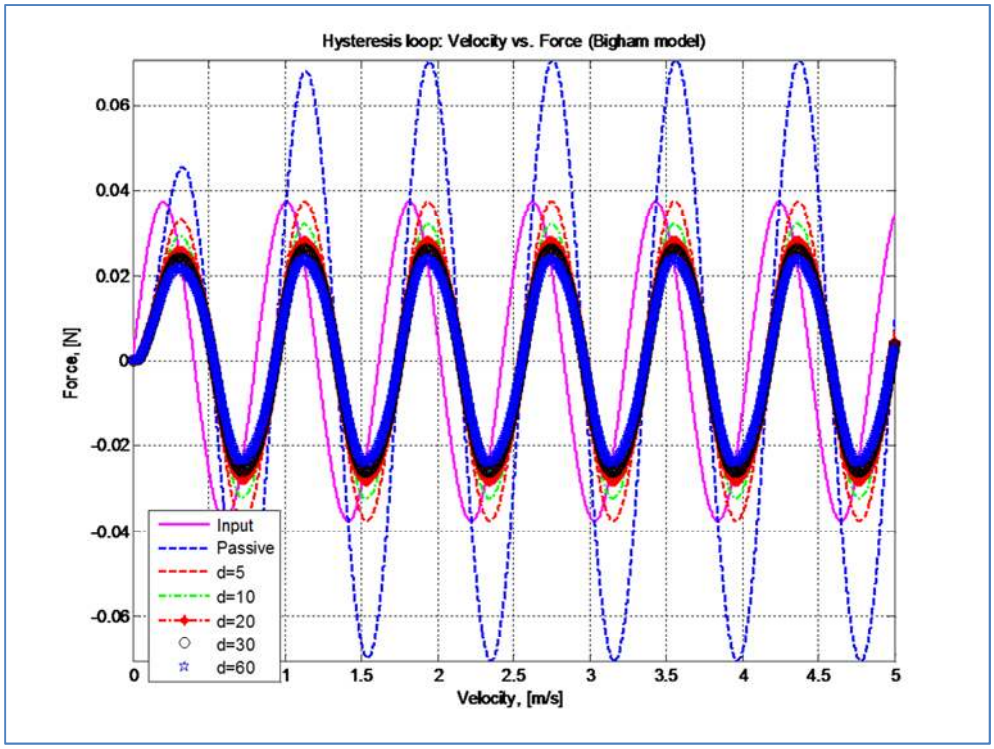

Figure 21. *The Bingham model responses on sine wave (with 7.77 rad/sec) excitation with different values of the form factor d.*

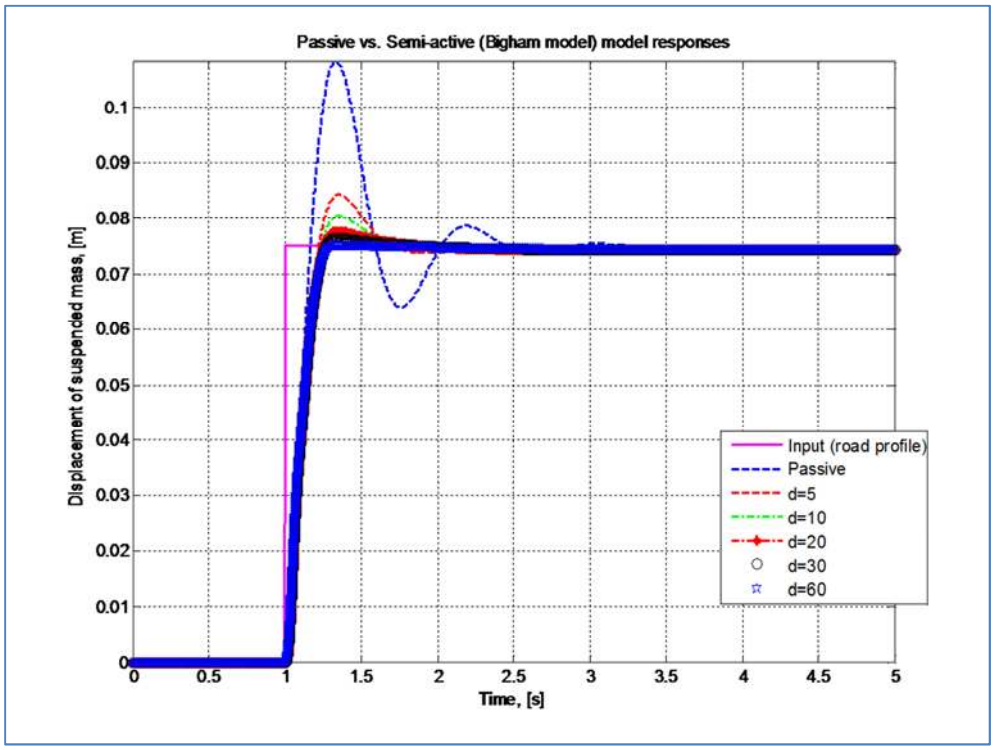

Figure 22. *The Bingham model responses on the Heaviside step excitation with different values of the form factor d.*

Similar to the Bingham model simulations, we have carried out several simulations for four different sets of hysteresis parameter values of the Dahl model. For example, Figure 23, 24 and 25 show how the dynamic hysteresis loop changes and the model responses for increasing values of all four hysteresis parameters or/and input voltage values alone when the input excitation signal is sine wave (with 67.3 rad/sec) and white Gaussian noise. By increasing four hysteresis parameter values, we obtain higher force generation but at the same time rather limited velocity change room. Besides, damping level of the undesired vibration on the suspended mass does not improve substantially by increasing the values of the hysteresis loops after certain values of the four parameters. However, we have not studied different values of each parameter individually with respect to others.

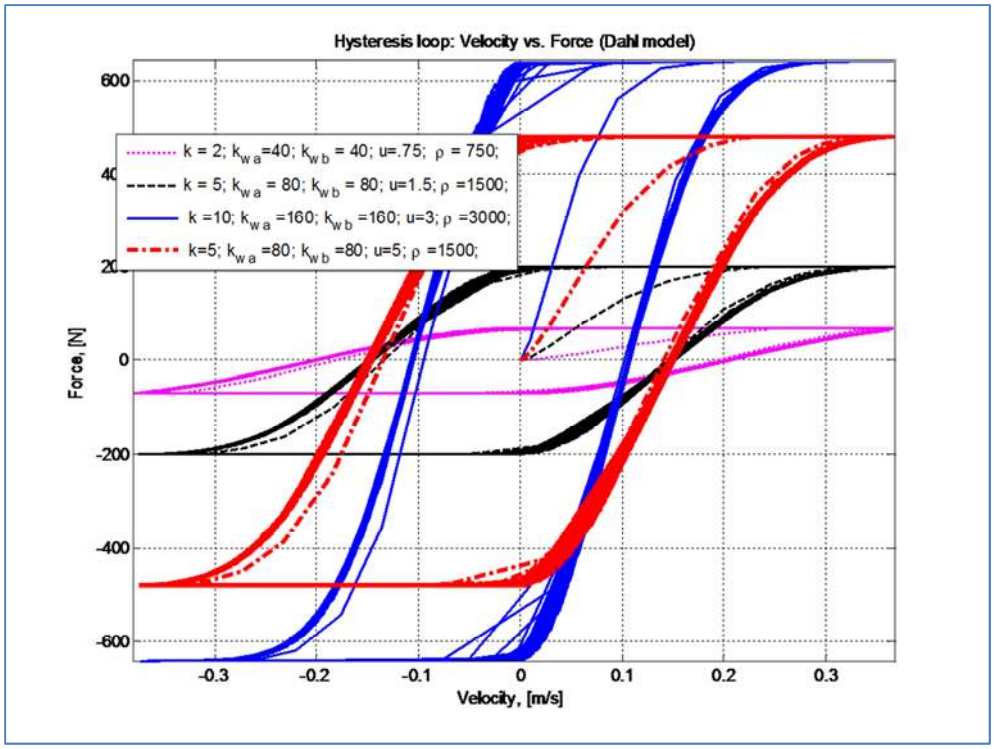

Figure 23. *The Dahl model response on pure sine wave (with 67.3 rad/sec) excitation.*

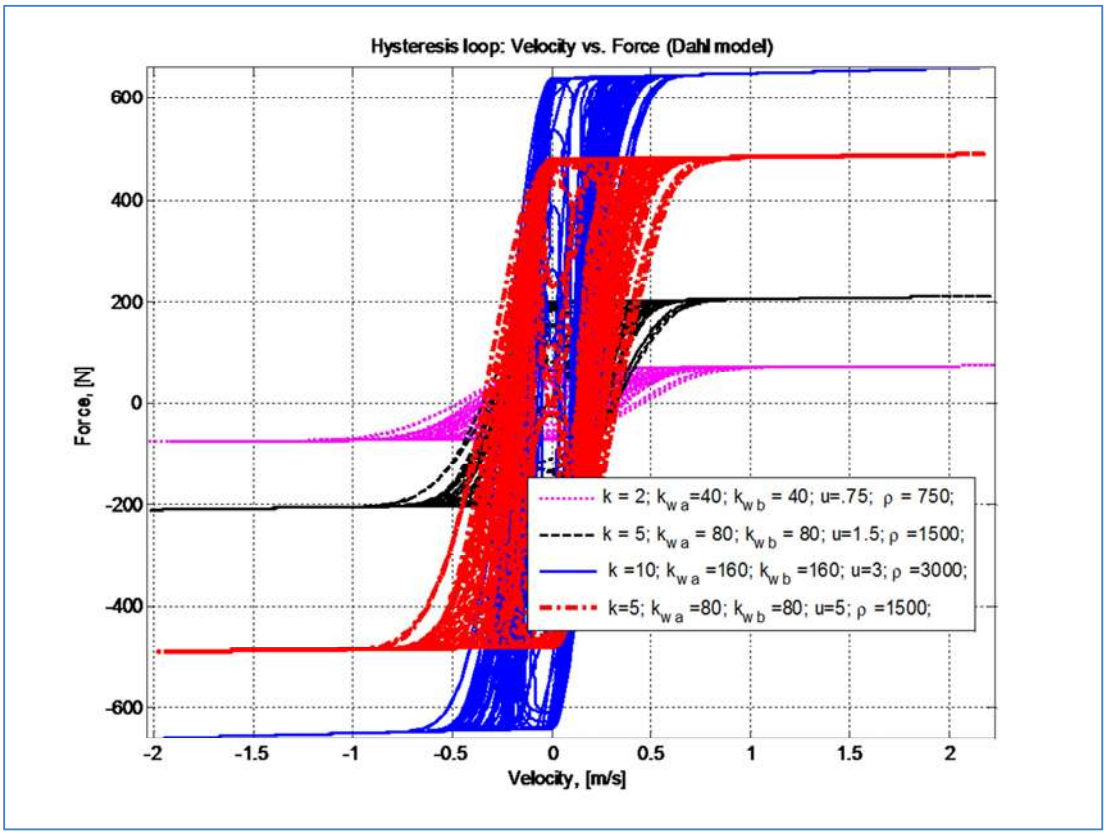

Figure 24. *Hysteresis loops of the Dahl model with input signal of white Gaussian noise.*

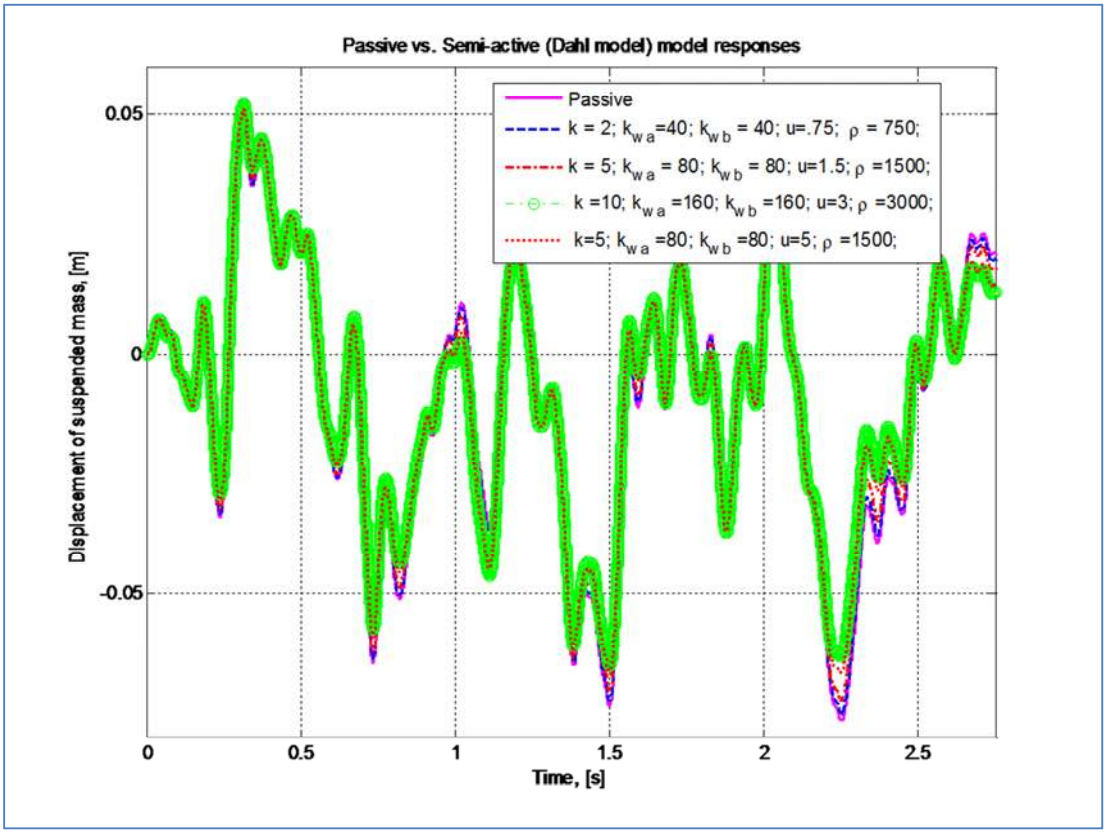

Figure 25. *The system responses on the white Gaussian noise.*

Simulations of the LuGre model with four different sets of hysteresis loop parameters (Figure 26 and 27) for the excitation signal of sine wave (with 7.77 rad/s) + white Gaussian noise (expressed in (14)) show that by increasing the values of the three parameters, viz. $\sigma_0, \sigma_1, \sigma_2$, we can attain higher values of the generated force with the cost of shrunk velocity value ranges. At the same time, efficiency of damping and responsiveness of the model appears to be considerable.

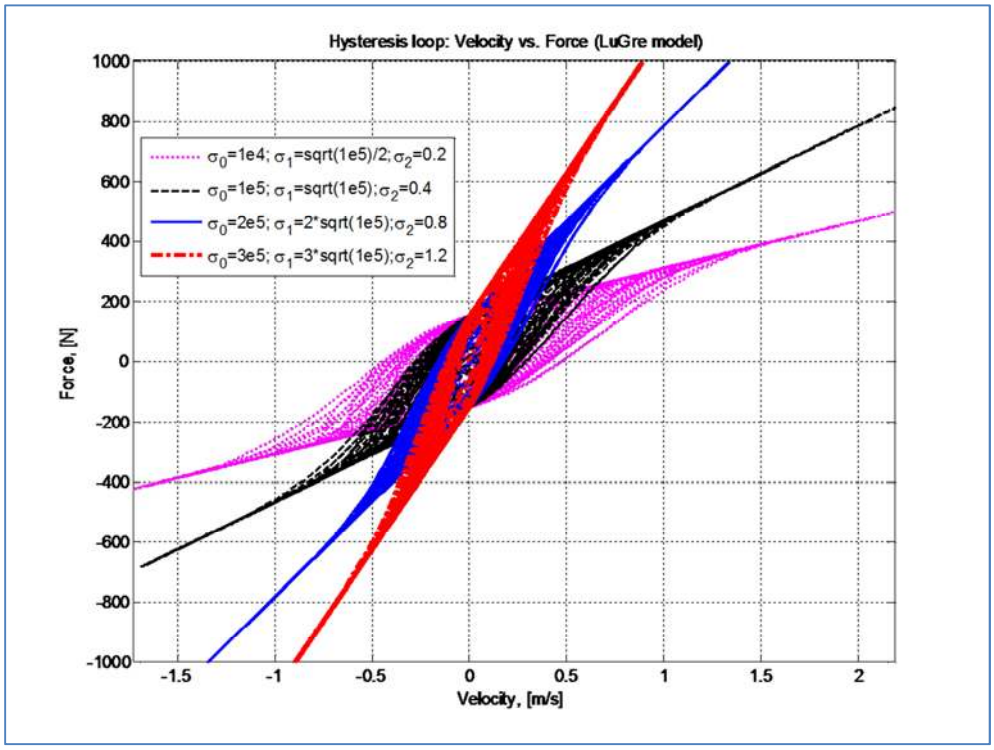

Figure 26. *Hysteresis loop of LuGre model with the input signal:* $0.0375 * sin(7.77 * 2 * \pi * t) + GWN$.

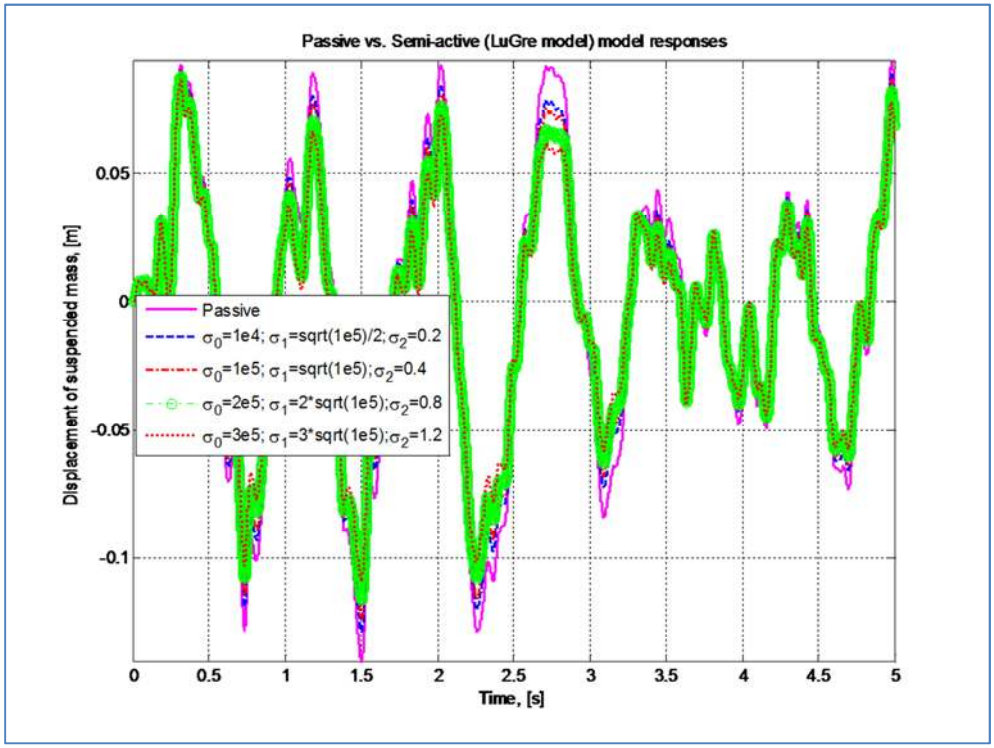

Figure 27. *The system responses: LuGre model with the input signal:* $0.0375 * sin(7.77 * 2 * \pi * t) + GWN$.

Similar to the other three models, we have also simulated the Bouc-Wen model's hysteresis loop parameters with four different sets of numerical values for the white Gaussian noise with 2.5 dBW power. The simulation results shown in Figure 28 and 29 demonstrate that unlike the other three models we can have much better control over the values of the hysteresis loop parameters and by changing its values we can enhance the performances of the model in terms of vibration damping efficiency and responsiveness of the model.

Another concluding remark from our comparative analysis of the four models and their performances with respect to value changes of hysteresis loop parameters is that performances of the all four models can be enhanced considerably by choosing or finding appropriate values for the parameters.

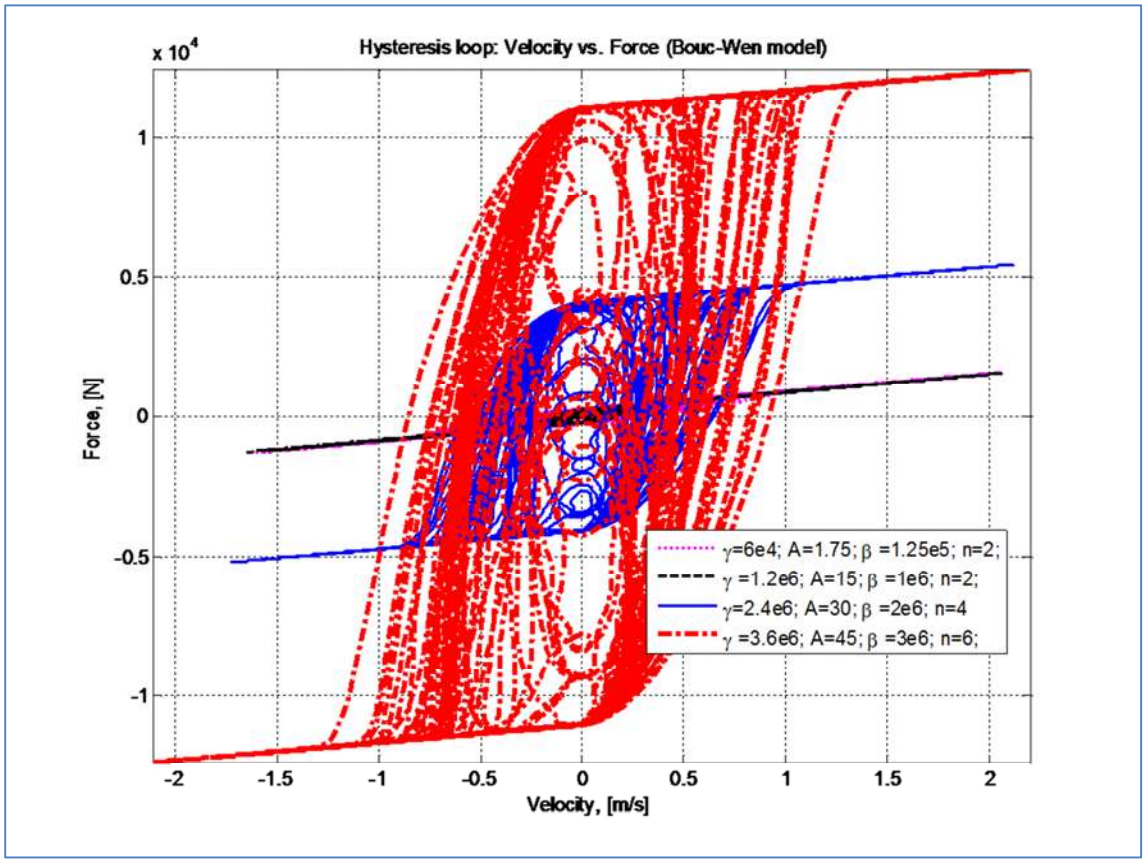

Figure 28. *Bouc-Wen model responses on white Gaussian noise excitation with 2.5 dBW power.*

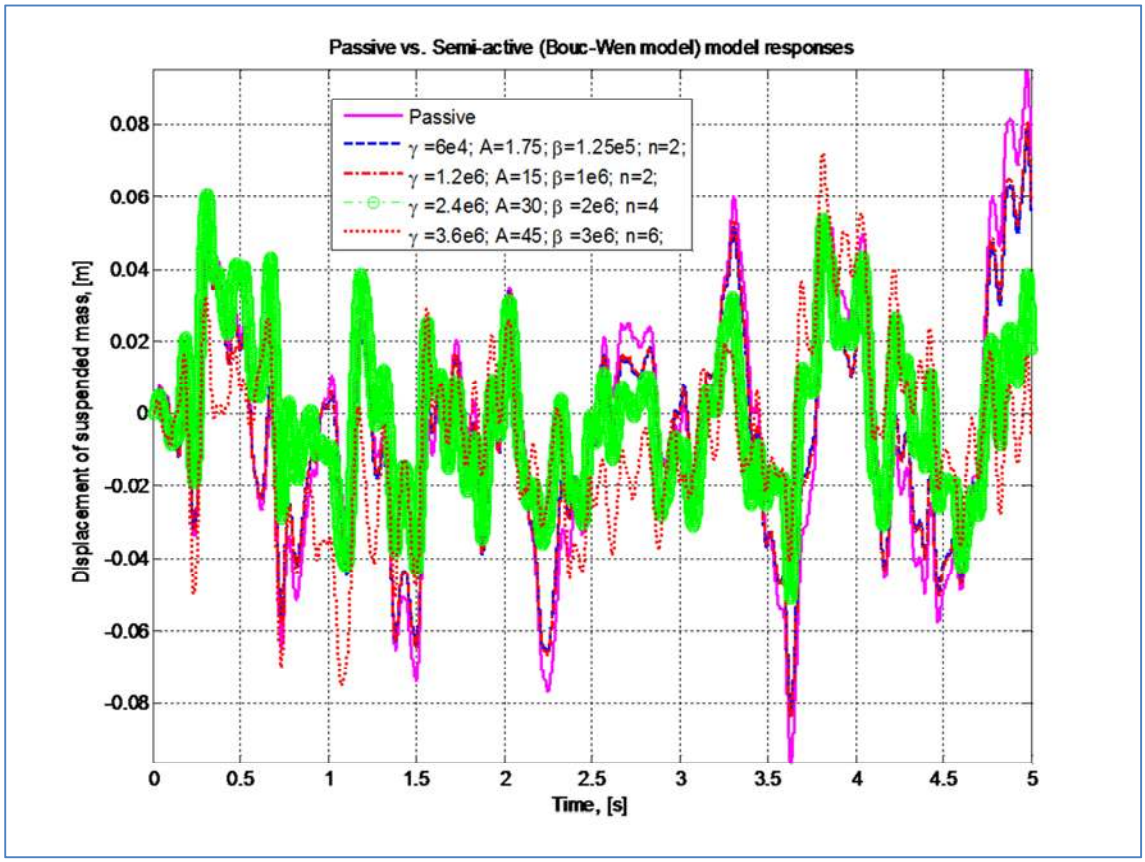

Figure 29. *Model responses (Passive vs. Bouc-Wen): on white Gaussian noise with the power of 2.5 dBW.*

5. Conclusions

The developed simulation models of the hysteresis or non-linear system behaviors of the MR liquids used in dampers via mathematical formulations of the Bingham, Dahl, LuGre and Bouc-Wen models in MATLAB®/Simulink® in the example of a quarter car model with the Golden Car parameters have showed adequacy of these MR dampers for designing vibration and shock dampers for vehicles. Based on the performed numerical simulations, we can conclude that all of the four models can provide enhanced and useful features of the dynamic hysteresis loop characteristics of the non-Newtonian liquids like the MR liquids used for dampers. In terms of better and enhanced control over the useful characteristics of non-linear features of the MR dampers, the Bouc-Wen model is more powerful and takes into account more properties and behaviors of hysteresis loops. On the other hand, the simpler model – Bingham model performs much better than the Bouc-Wen model for constant value excitations, such as, the Heaviside step function.

The simulation results of the semi-actively controlled damper designs with the Bingham, Dahl, LuGre and Bouc-Wen models have demonstrated considerably higher efficiency, faster response and higher performance over a passively controlled damper model for step, random noise, and low frequency sine wave signals mimicking terrain roughness. Their operational voltage is considerably low and energy efficiency is high at the same time. On the other hand, the efficiency of the MR damper models for higher frequency sine (periodic) wave excitations with and without Gaussian noises has been marginal. From our performed numerical simulations it is clear that efficiency and performance of the MR damper based on the all four models depend on the hysteresis loop parameters. Even though we have located some rational values of hysteresis loops in each model by trials and errors, but further studies are necessary to research the influence of each parameter with respect to others and find optimal parameter values. Therefore, our further studies will be aimed to develop mathematical (empirical) formulations and experimental validations to compute optimal parameters of the MR hysteresis based dampers with the modified Bingham, Dahl, LuGre and Bouc-Wen models with respect to vehicle suspension and tire parameters. Further studies will be also dedicated to develop an adaptive PID controller in association with these MR damper models.

Acknowledgements

This research is supported by the state grant # A-3-54 from the State Science and Technology Committee of Uzbekistan.

References

[1] Mitu A. M., Popescu I., Sireteanu T. (2012), "Mathematical modeling of semi-active control with application to building seismic protection," BSG Proceedings, Vol. 19, 2012, pp. 88-99.

[2] Sarkar Chiranjit and Hirani Harish (2015), "Synthesis and Characterization of Nao Silver Particle-based Magnetorheological Fluids for Brakes," Defence Science journal, Vol. 65, No. 3, May 2015, pp. 252-258.

[3] Sapinski B. (2009) "Magneto-rheological dampers in vibrational control of mechanical structures," Mechanics Vol. 28, No 1. 18-25 pp.

[4] Braz Cesar M., R. Carneiro de Barros R. (2012), "Properties and Numerical Modeling of MR dampers," 15th international conference on experimental mechanics, Porto, Portugal.

[5] Zhang H., et al. (2004), "Study on the design, test and simulation of a MR damper with two-stage electromagnetic coil," www.paper.edu.cn – viewed on March 13, 2016.

[6] Eshkabilov S., Grimheden M. E. (2015), "Car seat damper controller design with magneto-rheological fluids," Int. Conf., Nov., 2015, Navoi, Uzbekistan.

[7] Lee T. Y., Kawashima K., Chen P. C. (2008), "Experimental and Analytical Study on a Nonlinear Isolated Bridge under Semi-active Control", 14th World Conference on Earthquake Engineering, October 12-17, 2008, Beijing, China.

[8] Jolly M. R., Al-Bender B. F., and Carlsson J. D. (1999), "Properties and applications of commercial magneto-rheological fluids." Journal of Intelligent Materials Systems and Structures, 10 (1): 5-13.

[9] Stanway R., Sproston J. L., and Stevens N. G. (1987), Non-linear modelling of an electro-rheological vibration damper. Journal on Electrostatics, 20: 167-184.

[10] Dahl P. R. (1968), A solid friction model. Technical Report, TOR-158(3107-18) (El-Segundo, CA: The Aerospace Corporation).

[11] Canudas de Wit C, Olsson H. J., Astrom K. J., Lischinsky P (1993), Dynamics friction models and control design. American Control Conference, San Francisco, USA, pp. 1920-1926.

[12] Canudas de Wit C., Olsson H., Astrom K. J., and Lischinsky P. (1995), "A new model for control of systems with friction," IEEE Trans. Autom. Contr., vol. 40, no. 3, pp. 419–425.

[13] Bouc R. (1967), Forced vibrations of mechanical systems with hysteresis, Proceeding of the 4th Conference on Nonlinear Oscillations, Prague, Czechoslovakia 315-321.

[14] Wen Y. K. (1976), Method for random vibration of hysteretic systems, Journal of the Engineering Mechanics Division, 102 (2) (1976) 249-263.

[15] Spencer B. F. Jr., Dyke S. J., Sain M. K. and Carlson D. (1997), Phenomenological model of a magnetorheological damper, Journal of Engineering Mechanics ASCE, 123 (3) (1997) 230-238.

[16] Mat Hussain Ab Talib, Intan Z. Mat Darus (2013), "Self-tuning PID Controller with MR damper And Hydraulic Actuator For Suspension System", Fifth International Conference on Computational Intelligence, Modelling and Simulation, IEEE-Computer Society, DOI 10.1109/CIMSim.2013.27, pp. 119-124.

[17] Lampaert V., Al-Bender F. (2003), "A generalized Maxwell slip friction model appropriate for control purposes," IEEE – Physics Conference, St. Petersburg, Russia, pp. 1170-1177.

[18] Nguyen B. D., Aldo A. F., Olivier A. B. (2007), "Efficient Simulation of a Dynamic System with LuGre Friction," Journal of Computational and Nonlinear Dynamics, Vol. 2, pp. 281-289.

[19] Armstrong-H´elouvry B. (1991), “Control of Machines with Friction.” Boston, MA: Kluwer, 1991.

[20] Ikhouane F., Rodellar J. (1987), “Systems with hysteresis: analysis, identification and control using the Bouc-Wen model.” Wiley, Chichester (UK), 1987.

[21] Gillespie, T. D., Sayers, M. W., and Segel, L. (1980), “Calibration of Response-Type Road Roughness Measuring Systems.” Journal: National Cooperative Highway Research Program Report. No. 228, December 1980.

[22] Loizos, A., Plati C. (2008), Evolutional Process of Pavement Roughness Evaluation Benefiting from Sensor Technology, International Journal on Smart Sensing and Intelligent Systems, Vol. 1, No 2, June 2008, pp. 370-387.

[23] Ahlin K., Granlund J. (2001), International Roughness Index, IRI, and ISO 2631 Vibration Evaluation, Transportation Research Board: Committee on Surface Properties - Vehicle Interaction, Washington DC, January 2001.

Biography

Sulaymon L. Eshkabilov. He got ME from Tashkent Institute of Automotive Road Design, Construction and Maintenance (TIARDCM) in 1994, earned MSc from Rochester Institute of Technology in 2001 and PhD from Cybernetics research Institute of Academy Sciences of Uzbekistan in 2005. He was a visiting professor in 2010-2011 at Mechanical Engineering department of Ohio University, OH, USA. He is currently an associate professor at TIARDCM and holds a part-time professor position at Tashkent-Turin Polytechnic University. His research areas are mechanical vibrations and applications of modal analysis, system identification, control and modeling of dynamic systems.